# PHYSICOCHEMICAL PROPERTIES OF INDOOR AND OUTDOOR PARTICULATE MATTER IN RESIDENTIAL AREAS NEAR A FERROMANGANESE SMELTER

UNIVERSITY OF THE
WITWATERSRAND,
JOHANNESBURG


Setlamorago Jackson Thobejane

Student number: 2281450

Supervisor: Dr Masilu Daniel Masekameni
Faculty of Health Sciences, School of Public Health, Occupational Health Division
University of the Witwatersrand


A research report submitted in the Faculty of Health Sciences, University of the Witwatersrand, Johannesburg in partial fulfilment of the requirements for the degree of Master of Science in Medicine (Exposure Science)

June 2021

# Declaration

I, **Setlamorago Jackson Thobejane (student number: 2281450)** declare that the research project entitled *"Physicochemical Properties of Indoor and Outdoor Particulate matter in a Residential Area Near a Ferromanganese Smelter"* is my research work undertaken under the supervision of Dr Masilu Daniel Masekameni. The work is being submitted in partial fulfilment for the degree of Master of Medicine in the field of Exposure Science at the School of Public Health, University of the Witwatersrand, Johannesburg. This work has not been presented for examination at any other university. The author designed the study, conducted all field data collection, data analysis, and writing the research report. Parts of this research report have been planned to be published in peer-reviewed journals and presented at conferences. All the sources cited in this study have been acknowledged through comprehensive references. The senate plagiarism policy is signed and attached as Appendix A: Plagiarism Declaration Form.

**Abstract submission**

Thobejane, SJ., Masekameni, MD. "Physicochemical properties and relationship between indoor and outdoor particulate matter in residential areas near a ferromanganese smelter". 12th Wits Cross-Faculty Postgraduate Symposium 2021.

**Targeted conference**

Thobejane, SJ., Masekameni, MD., Nelson G. "Physicochemical properties and relationship between indoor and outdoor particulate matter in residential areas near a ferromanganese smelter". National Association on Clean Air 2021 conference.

**Manuscripts in preparation**

1. Thobejane, SJ., Masekameni, MD., Nelson G. "Physicochemical properties and relationship between indoor and outdoor particulate matter in residential areas near a ferromanganese smelter".
2. Thobejane, SJ., Masekameni, MD. "Human health risk assessment of indoor and outdoor heavy metals in a residential area downwind of a ferromanganese smelter"
3. Thobejane, SJ., Masekameni, MD. "Source apportionment of indoor and outdoor particulate matter in a residential area near a ferromanganese smelter using chemical mass balance and positive factorisation matrix"

# Dedication

This research report is dedicated to my family for the endless support they have given me in good and bad times. I appreciate the support that my sisters (Melita, Mahlako, Mathodi, Refilwe, Thobejane, and Neria Mbazima) have given me and the encouragement that my brothers (Seremi and Bauba Thobejane) have I would also like to thank my partner Yonda Nokhwethu for the understanding and support that she has provided throughout the years and for having patience when I was a present but absent partner. Lastly, to my newborn child Atamelang, welcome to earth my son!

# Abstract


## Background

Approximately 90% of the world's population resides in areas where ambient air quality standards are exceeded. Particulate matter with an aerodynamic size of less than 2.5 µm ($PM_{2.5}$) has been identified as the leading contributor to indoor and outdoor air pollution. $PM_{2.5}$ can be released from natural and anthropogenic sources, however, anthropogenic sources such as ferromanganese smelters are among the major sources. Ferromanganese smelters tend to release Mn-bearing $PM_{2.5}$. Owing to their size, Mn-bearing $PM_{2.5}$ can remain suspended for longer periods and travel a greater distance from the emitting source and penetrate indoor environments. It is suggested that most people, especially vulnerable groups spend approximately 80%–90% of their time indoors. Chronic exposure to Mn-bearing $PM_{2.5}$ is associated with neurological disorders. Most of the evidence on the causal relationship between Mn exposure and neurological disorder was drawn from epidemiological studies that lacked exposure assessments.

## Purpose

To systematically characterise the similarities between indoor and outdoor $PM_{2.5}$ airborne particles in residential areas within the vicinity of the smelter in Meyerton.

## Methods

Indoor and outdoor airborne $PM_{2.5}$ were collected concurrently from selected households using two identical active samplers. A gravimetric sampling technique was used to sample $PM_{2.5}$ continuously over seven days from the 30 selected households. GilAir plus pumps were used to draw in air containing $PM_{2.5}$ into the sampling media at a flow rate of 2.75 L/min. The sampling media comprised of a 37 mm cassette, which was housed in a 37 mm polycarbonate filter. A 1.5 m long Teflon tubing was used to connect the sampling media outlet to the inlet of the pump. A total of 60 samples were collected over three months (August–November 2019) and comprised 30 indoor and 30 outdoor samples. $PM_{2.5}$ mass concentrations were obtained gravimetrically using a microbalance scale. The physicochemical properties were analysed using scanning electron microscopy coupled with energy-dispersive X-ray spectroscopy (SEM-EDX). Inductively coupled plasma-mass spectrometry (ICP-MS) was used to analyse the elemental composition of indoor and outdoor $PM_{2.5}$. The difference between indoor and outdoor $PM_{2.5}$ mass concentration was

determined by calculating the indoor-outdoor ratio, where a ratio greater than 1 indicated that indoor $PM_{2.5}$ is less than the outdoor. Furthermore, statistical analysis for indoor and outdoor $PM_{2.5}$ was performed using an F-Test and a Student t-test. A P-value of <0.05 indicated a statistically significant difference between indoor and outdoor $PM_{2.5}$.

**Results**

Indoor $PM_{2.5}$ mass concentration ranged between 2.88 and 19.19 µg/m$^3$ with an average of 10.99 ± 5.10 µg/m$^3$ while outdoor concentration ranged between 11.68 and 40.44 µg/m$^3$ with an average of 24.97 ± 6.77 µg/m$^3$. Outdoor $PM_{2.5}$ mass concentration in Meyerton was 2.7 fold greater than the indoor. The I/O ratio of $PM_{2.5}$ was 0.44 indicating that indoor $PM_{2.5}$ was lower than the outdoor. The I/O ratio of less than 1 further indicated and that indoor $PM_{2.5}$ was influenced by PM from the outdoor environment. A statistically significant difference was found ($P$=5.8×10$^{-13}$) between indoor and outdoor $PM_{2.5}$ mass concentrations. SEM images showed that indoor $PM_{2.5}$ consisted of irregular and agglomerated particles ranging from 0.1 to 0.7 µm in diameter while $PM_{2.5}$ outdoor also consisted of irregular but single spherical particles ranging from 0.1 to 1.3 µm in diameter. SEM images showed similarities between indoor and outdoor particles suggesting that they are from the same or similar source. ICP-MS results indicated an abundance of elements in decreasing order of Si > Fe > Zn > Mn both on indoor and outdoor $PM_{2.5}$. However, outdoor $PM_{2.5}$ had the highest concentration of Mn, Zn, Si, and Fe relative to indoor $PM_{2.5}$. The average indoor and outdoor Mn concentration was 1.30 µg/m$^3$ and 5.36 µg/m$^3$, respectively.

**Conclusion**

This study investigated the similarities between the physicochemical properties of indoor and outdoor $PM_{2.5}$ sampled in residential areas near a ferromanganese smelter and found that most indoor $PM_{2.5}$ originated from an outdoor source. Moreover, indoor and outdoor $PM_{2.5}$ were enriched with Mn and other elements, which can lead to chronic health outcomes amongst vulnerable groups. Since Mn and the other elements found in this study are mainly released from ferromanganese smelters, the nearby smelter might be a major source of indoor and outdoor Mn-bearing $PM_{2.5}$ in Meyerton. However, further studies using advanced source apportionment techniques are recommended to verify the findings. Lessons drawn from this study suggest the need for integrated town planning and development where ferromanganese smelter are not supposed to be built near residential areas. Measures such as tree plantation may be introduced in such residential areas to reduce or trap airborne PM.

# Acknowledgements

I am indebted to several individuals who have made this study possible. My sincere gratitude goes firstly to my supervisor Doctor Masilu Daniel Masekameni who has been more than a mentor from the beginning. I am grateful for the support patience, guidance, and encouragement that has given me through my academic years and for making me relevant. I am privileged to have a supervisor of your calibre who is approachable and cared more about my work and well-being and answered my questions and queries sufficiently no matter the time of the day. Thank you very much for sacrificing your family time for this project, your invaluable guidance has truly helped me develop individually and professionally. It has been a great experience of learning and cross-fertilisation of ideas. Above all, thank you for teaching me that the fruit of your hard work is the sweetest.

I would also like to thank Professor Gill Nelson, Professor Jay Turner, and Doctor Brad Racette for allowing me to partake in this research project, thank you for the opportunity, and for having faith in me. I am also indebted to Mr. Tony Da Silva for assisting during the fieldwork. I am grateful to Mrs. Jeanneth Manganyi from the National Institute of Occupational Hygiene for her support with sampling equipment. Thank you to Doctor Daniel Mmereki for lending support where needed. I would also like to thank Mr. Siyasanga Mpesane for his assistance with the SEM-EDX analysis and Mr. Philip Pieterse for his assistance with the ICP-MS analysis. Lastly, thank you to all the study participants for their co-operation and for allowing us into their households, this project would have never been a success with you.

# Table of Contents

# Nomenclature

## List of abbreviations

| | |
|---|---|
| **AG** | Atkiengesellschaft |
| **Al** | Aluminium |
| **Amcor** | African Metals Cooperation Limited |
| **As** | Arsenic |
| **ATSDR** | Agency for Toxic Substances and disease registry |
| **BSE** | Back-scattered electron |
| **Ca** | Calcium |
| **Cd** | Cadmium |
| **CNS** | Central nervous system |
| **Co** | Cobalt |
| **Cr** | Chromium |
| **Cu** | Copper |
| **EDX** | Energy-dispersive X-ray spectroscopy |
| **Fe** | Iron |
| **FeMn** | Iron Manganese |
| **FeSi** | Ferrosilicon |
| **FeTi** | Ferrotitanium |
| **FeW** | Ferrotungsten |
| **FL** | Florida |
| **GPS** | Global positioning system |
| **$H_2O_2$** | Hydrogen peroxide |
| **HCFeMn** | High-carbon ferromanganese |
| **$HNO_3$** | Nitric acid |
| **I/O** | Indoor-outdoor ratio |

| | |
|---|---|
| **ICP-MS** | Inductively coupled plasma-mass spectrometry |
| **K** | Potassium |
| **LCFeCr** | Low-ferrochromium |
| **LCSiMn** | Low-carbon silicomanganese |
| **LoD** | Limit of detection |
| **LoQ** | Limit of quantification |
| **MCFeCr** | Medium-ferrochromium |
| **MCFeMn** | Medium-carbon ferromanganese |
| **Mg** | Magnesium |
| **MMT** | Methylcyclopentadienyl manganese tricarbonyl |
| **Mn** | Manganese |
| **MnDPDP** | Mangafodipir trisodium |
| **MRI** | Magnetic resonance imaging |
| **Na** | Sodium |
| **Ni** | Nickel |
| **Pb** | Lead |
| **PCTE** | Polycarbonate membrane |
| **PD** | Parkinson's disease |
| **PM** | Particulate matter |
| **$PM_{2.5}$** | Particulate matter less than 2.5 in diameter |
| **S** | Sulphur |
| **SD** | Standard deviation |
| **SE** | Secondary electron |
| **SEM** | Scanning electron microscopy |
| **SEM-EDX** | Scanning electron microscopy coupled with energy dispersive X-ray |
| **Si** | Silicon |

| | |
|---|---|
| **SiMn** | Silicomanganese |
| **UK** | United Kingdom |
| **USA** | United States of America |
| **V** | Vanadium |
| **WHO** | World Health Organization |
| **Wt%** | Weight percent |
| **Zn** | Zinc |

## SI units and symbols

| | |
|---|---|
| **%** | Percent |
| **ºC** | Degree Celsius |
| **µg** | Microgram |
| **µg/L** | Microgram per litre |
| **µg/m$^3$** | Microgram per cubic metre |
| **µm** | Micrometer |
| **C** | Concentration |
| **$C_e$** | Element concentration |
| **cm$^2$** | Square centimetre |
| **g** | Gram |
| **kg** | Killogram |
| **km** | Kilometre |
| **km/h** | Kilometre per hour |
| **km$^2$** | Square kilometre |
| **kV** | Kilovolt |
| **L/min** | Litres per minute |
| **m** | Mass |
| **m** | Metre |

| | |
|---|---|
| **$m^3$** | Cubic metre |
| **$M_e$** | Element mass |
| **mg/L** | Milligram per litre |
| **$mg/m^3$** | Miligram per cubic metre |
| **mL** | Millilitres |
| **mm** | Millimeter |
| **MVA** | Mega volt-ampere |
| **$M\Omega/cm^2$** | Milliohm per square centimetre |
| **nA** | Nanoampere |
| **$ng/m^3$** | Nanogram per cubic metre |
| **nm** | Nanometre |
| **V** | Volume |

# List of Figures

# List of Tables

# CHAPTER 1: INTRODUCTION

This chapter begins with an overview of particulate matter (PM) and its natural and anthropogenic sources and their impact on indoor and outdoor air quality. The release of Manganese-bearing PM from ferromanganese smelters is outlined and the chapter further describes Manganese as a trace element and micronutrient, its use, and the health outcomes associated with exposure to Mn-bearing PM. The problem statement and justification of the study are outlined and the chapter ends by presenting the study aim, hypothesis, and objectives.

## 1.1 Background

Particulate matter (PM) refers to a mixture of particles suspended in the air in a liquid or solid form which are often observed as dust, smoke, or haze (Brüske-Hohlfeld and Peters, 2010; Lowther *et al.*, 2019). PM is categorised into $PM_{0.1}$ (<0.1 μm), $PM_{2.5}$ (<2.5 μm), and $PM_{10}$ (<10 μm) depending on the aerodynamic diameter (Brüske-Hohlfeld and Peters, 2010; Hoeflinger and Laminger, 2019). The World Health Organization (WHO), stated that approximately 90% of the global population has no access to clean air (World Health Organization, 2016).

The WHO further stated that most people reside in areas where ambient air quality standards are exceeded (World Health Organization, 2016) and $PM_{2.5}$ has been identified as the leading contributor to indoor and outdoor air pollution (Li *et al.*, 2017). $PM_{2.5}$ has been categorised as a criteria pollutant by the South African National Standards (Gholampour *et al.*, 2016) and it is used as an indicator of air pollution globally (Hänninen and Goodman, 2019).

$PM_{2.5}$ can be emitted from various sources (Pöschl, 2010), the sources are classified into two main categories, natural and anthropogenic sources (Ahmed, Guo and Zhao, 2017; Galvão *et al.*, 2018). Natural sources associated with the release of $PM_2$ include cyclones, earthquakes, and uranium decay (Mukherjee and Agrawal, 2017; Galvão *et al.*, 2018). Anthropogenic sources include industrial activities, residential areas, and automobiles, however, compelling literature highlights industrial activities as major sources of $PM_{2.5}$ (Galvão *et al.*, 2018).

Electricity generation, ferromanganese smelters, metal casting, and mining activities are among the leading sources in the industrial sector that contribute to $PM_{2.5}$ emissions with

different physicochemical properties (Sielicki *et al.*, 2011; Gonzalez-Castanedo *et al.*, 2014; Zhou *et al.*, 2019). Such activities operate at a high temperature and often release single particles with an aerodynamic diameter of 1 μm or less, also known as submicron PM (Valavanidis, Fiotakis and Thomas, 2008; Masekameni *et al.*, 2018).

Ferromanganese smelters are some of the industrial activities operated at temperatures between 100 and 1 400ºC (Marris *et al.*, 2012) resulting in the emission of submicron PM (Lighty, Veranth and Sarofim, 2000). Ferroalloy production processes such as raw material and product handling, sintering, smelting, tapping, and casting release Mn-bearing PM with different physicochemical properties (Davourie *et al.*, 2017; Hernández-Pellón *et al.*, 2017). The Mn-bearing PM may also have high concentrations of elements such as lead (Pb), Mercury (Hg), Cadmium (Cd), Nickel (Ni), Arsenic (As), and Chromium (Cr) (Mazzei *et al.*, 2008; Li *et al.*, 2017). These elements are commonly found in the environment and have similar neurotoxic effects (Popoola *et al.*, 2018).

Submicron PM has a higher resident time in the atmosphere and can be easily be transported over a greater distance from the initial source of release (Hernández-Pellón and Fernández-Olmo, 2019; Lowther *et al.*, 2019). During transportation, the particles tend to undergo a chemical and physical transformation and grow into larger particles with an aerodynamic diameter of 2.5 μm or less by the time they reach a residential area (Galvão *et al.*, 2018; Thompson, 2018).

The particles grow from nucleation or Aitken (0.0001–0.1 μm), accumulation mode (0.1–2.5 μm), and to course mode (2.5–10 μm) due to agglomeration, condensation, and accumulation (Riffault *et al.*, 2015; Rohra *et al.*, 2018), and they agglomerate based on their inherent chemical and physical characteristics (Setyan *et al.*, 2019; Zhou *et al.*, 2019). Furthermore, $PM_{2.5}$ moves and deposit through diffusion relative to larger particles ($PM_{10}$) that deposit through gravitational force (Morawska *et al.*, 2013).

The deposited PM can settle on a residential building and enter indoor environments through infiltration, filtration, foot tracking, open windows, and other openings. The indoor-outdoor (I/O) ratio can be used to determine the relationship between indoor and outdoor PM mass concentrations (Martins *et al.*, 2020). An I/O ratio of less than 1 indicates good indoor air quality and the absence of major indoor contributing sources (Chen and Zhao, 2011; Martins *et al.*, 2020) while an I/O ratio greater than 1 indicates a presence of significant indoor sources (Pallarés *et al.*, 2019). In the absence of major indoor sources, indoor air quality is directly linked to outdoor sources (Guo *et al.*, 2010).

Although the size and morphology determine the fate of the PM in the respiratory tract (Allen *et al.*, 2017), however, the elemental composition also affects health outcomes (Galvão *et al.*, 2018). Therefore, information and understanding of the physicochemical properties are needed to apportion the source and protect public health since atmospheric PM is a complex mixture and the elemental composition differs (Peters *et al.*, 2006; Rodríguez *et al.*, 2007; Park *et al.*, 2018). Due to the complexity of PM, elemental isolation within a mixture is necessary to determine the potential for source contribution and possible health effects (Genga *et al.*, 2018).

It is well established that ferromanganese smelters release a significant amount of Mn-bearing PM into the atmosphere (Bowler *et al.*, 2016). Due to the inherent risks associated with Mn exposure (Racette *et al.*, 2018), it is necessary to establish the relationship between indoor and outdoor PM levels using Mn as an indicator element.

## 1.2 Literature review

Mn exists in an organic and inorganic form and it is the fifth most abundant heavy metal and the twelfth most abundant trace element in the earth's crust (Horning *et al.*, 2015; O'Neal and Zheng, 2015). Mn comprises approximately 0.1% of the earth's crust and commonly exists as oxides, carbonates, and silicates (Chen, Culbreth and Aschner, 2016). It also occurs naturally in certain food products, however, it can be added as a nutritional supplement (Horning *et al.*, 2015). It can be found in food products such as legumes, rice, nuts, whole grains, seafood, and teas (Peres *et al.*, 2016). Levels between 2 and 5 mg/day and 9 and 11 mg/day are regarded as a sufficient daily intake for children and adults respectively (Aschner and Aschner, 2005; Miah *et al.*, 2020).

At an acceptable daily intake, Mn is essential for human physiological functions such as bone mineralization, metabolic regulation, and breakdown of cholesterol, carbohydrates, and proteins (Menezes-Filho *et al.*, 2014; Verenice Muñoz-Rocha *et al.*, 2018; dos Santos *et al.*, 2019). Due to its catalytic and regulatory functions, Mn is important in biochemical reactions of several enzymes including Mn-dependent superoxide dismutase (Michalke and Fernsebner, 2014). Also, Mn maintains the nervous and immune system and it is necessary for normal reproductive hormone function and the prevention of cellular oxidative stress (Hernández-Pellón *et al.*, 2017; Hernández-Pellón and Fernández-Olmo, 2019).

Countries rich with Mn reserves are Gabon, South Africa, China, and Ghana (Chen, Culbreth and Aschner, 2016). South Africa reserves 80% of the world's high-grade Mn and it is the

largest producer of high-quality manganese (Steenkamp and Basson, 2013; Coetsee, 2019). The Mn reserves in South Africa are found in the Kalahari Basin, Northern Cape Province and the Kalahari Basin reserves 90% Mn which consists of the Mamatwan and Wessels type (Steenkamp and Basson, 2013). In 2001, 50% of the Mn ore mined in the country was smelted locally and the numbers have remained constant over the years (Steenkamp *et al.*, 2018).

### 1.2.1 Use of manganese

Manganese and its compounds are used in various industries for the production of steel, welding rods, fireworks, dry cell batteries, and various Mn chemical products (Otero-Pregigueiro and Fernández-Olmo, 2018; Ou *et al.*, 2018). In steel and stainless industries, Mn is a common and important constituent that is used as a supplement to improve the quality of the steel (Davourie *et al.*, 2017; Coetsee, 2019). Mn is primarily used for the deoxidisation and desulphurisation of the steel and to control the morphology of the sulphides and improve the strength, toughness, and hardness of the steel (Steenkamp and Basson, 2013).

Approximately two tonnes of Mn are required to produce 1 tonne of ferromanganese (ATSDR, 2012). Approximately 90% of the Mn ferroalloys produced are in the steelmaking making industry at a consumption rate between 7.5 and 10 kg of Mn per tonne of steel (Steenkamp and Basson, 2013). The sintering step generates fine particles relative to the other steps involved in the processing of Mn (Sammut *et al.*, 2010). Other than the application in Mn ferroalloys, Mn is also used in the production of Cu, Al, and Silver-Cu alloys and other non-metallic applications such as fertilisers and dry cell batteries production (Steenkamp and Basson, 2013).

After the ban of Pb in the petroleum industry, methylcyclopentadienyl manganese tricarbonyl (MMT) which is an organic derivative of Mn has been used significantly as an additive to improve the octane level and anti-knock of petrol (Beaupré *et al.*, 2004; Finkelstein and Jerrett, 2007; Walsh, 2007). Mn is also used in the production of pesticides and fungicides such as Mn ethylene-bis-dithiocarbamate (maneb) and dithiocarbamate (mancozeb) (Crossgrove and Zheng, 2004; Chen, Culbreth and Aschner, 2016). Due to its paramagnetic nature, mangafodipir trisodium (MnDPDP) is used as a liver and pancreas-specific contrasting agent for MRI (Aschner *et al.*, 2009; Chen, Culbreth and Aschner, 2016).

### 1.2.2 Sources of Mn-bearing PM

The sources of Mn-bearing PM can be divided into natural and anthropogenic sources. Crustal rock is a major natural source of atmospheric Mn-bearing particles. Mn-bearing PM can be released during ocean spray, forest fires, volcanic eruptions, and vegetation activities such as ploughing (Malcolm, Wood and Kingdom, 2004; Omrani *et al.*, 2017). However, natural sources emit coarse Mn-bearing particles relative to anthropogenic sources (Martins *et al.*, 2020).

Anthropogenic sources of Mn include municipal wastewater discharges, sewage sludge, mining and mineral processing, the combustion of fossil fuels, automobiles, battery and pesticides manufacturing alloy, steel, and iron smelters (Malcolm, Wood and Kingdom, 2004; Omrani *et al.*, 2017; Popoola *et al.*, 2018). Studies investigating the formation and release of PM from automobiles have been conducted. Karagulian *et al.* (2015), Amato *et al.* (2016) and (2017) reported that automobiles are significant contributors to atmospheric PM concentration levels in urban areas.

Automobiles became a contributing source of Mn-bearing particles due to the use of MMT (Walsh, 2007). The combustion of MMT in automobile engines leads to the formation and release of Mn-bearing particles in the size range between 0.2 and 10 µm (Loranger and Zayed, 1995). Although fuel combustion in automobiles is the predominant way in which PM is formed and released, the mechanical abrasion and corrosion processes such as tyre, clutch, and brake wear, and road surface abrasion also contribute to the formation and release of PM (Viana, 2013; Liati *et al.*, 2016; Alves *et al.*, 2020). Both the mechanical and exhaust-formed PM will settle on the road surface and can be suspended or resuspended due to wind and or automobile-generated turbulence (Viana, 2013). These processes are suggested to contribute significantly to the atmospheric $PM_{2.5}$ concentration levels (Alves *et al.*, 2020).

### 1.2.3 Exposure to Mn

Exposure to Mn can occur through three common routes, which are ingestion, dermal, and inhalation (Carvalho *et al.*, 2018; Oberdörster and Kuhlbusch, 2018). Ingestion can occur through the direct consumption of water and food containing Mn (Horning *et al.*, 2015). The dermal route exposure can occur when bathing using water that is contaminated with Mn or through contact with Mn-bearing particles, however, direct contact with the Mn-bearing PM is considered less effective (Jin *et al.*, 2018; Thompson, 2018). The inhalation route is considered the most obvious, effective, and susceptible route of entry relative to the ingestion

and dermal route (Menezes-Filho *et al.*, 2009; Otero-Pregigueiro and Fernández-Olmo, 2018).

The uptake of Mn-bearing PM through the inhalation route is considered threatening because Mn-bearing PM can bypass normal biliary excretion mechanisms and directly enter the brain along the olfactory neurons before it can be metabolized by the liver (Haynes *et al.*, 2010; Hernández-Bonilla *et al.*, 2011; Fulk *et al.*, 2017). Moreover, inhaled Mn can directly enter the CNS and be absorbed more effectively (Lee *et al.*, 2017; Riediker *et al.*, 2019). Some of the Mn-bearing PM will be absorbed by macrophages and transported into the systemic circulation causing systematic effects (Andruska and Racette, 2015; Salma *et al.*, 2015).

Exposure to Mn-bearing PM can occur indoor or outdoor¸ however, it has been argued that exposure to airborne particles mainly occurs indoors (Monn, 2002). This is concerning since it is suggested that in modern society, residents spend approximately 80%–90% of their time indoors (Manigrasso *et al.*, 2018; Koivisto *et al.*, 2019). The elderly, sick, pregnant women, and children spend most of their time indoors (Pavilonis *et al.*, 2015; Delgado-Saborit, 2019) and they are considered vulnerable because of their higher duration of exposure and a weak or compromised immune system (Zota *et al.*, 2011; Morawska *et al.*, 2013).

Exposure to Mn-bearing PM has been associated with neurological disorders, premature death, and respiratory illnesses globally (Cortez-Lugo *et al.*, 2018). Furthermore, Mn-bearing $PM_{2.5}$ can be deposited in the bronchi and penetrate deeper into the alveoli during gaseous exchange (Andruska and Racette, 2015; Hu *et al.*, 2015). To better understand the potential exposure and health outcomes in residents living near a ferromanganese smelter, it is important to assess the similarities between indoor and outdoor PM concentrations and their physicochemical properties (Sajani *et al.*, 2015).

### 1.2.4 Health effects of Manganese

Although Mn plays a vital role in human physiological functions, exposure to excessive levels of Mn can result in adverse neurotoxic health effects (Fulk *et al.*, 2017; Kornblith *et al.*, 2018). Environmental exposure to Mn-bearing PM is associated with neurological health effects (Colledge *et al.*, 2015; Kornblith *et al.*, 2018). In addition, studies (Smith *et al.*, 2007; Menezes-Filho *et al.*, 2009; Cantone *et al.*, 2011; Nascimento *et al.*, 2016; Hernández-Pellón *et al.*, 2017; Rodrigues *et al.*, 2018) have confirmed and reported a consistent and significant association between exposure to airborne Mn-bearing PM and manganism and other

neurobehavioral deficits at low concentration levels in residential areas near ferromanganese smelters.

The biological mechanisms by which Mn exerts its toxicity on humans have not yet been fully understood, however, chronic exposure to Mn-bearing PM has been associated with CNS disorders (Rodrigues *et al.*, 2018). Mn accumulates in the brain and enters the CNS where it is absorbed more effectively. Once Mn is absorbed in the CNS, it causes adverse effects on the basal ganglia leading to a neurologic psychiatric disorder known as manganism which is similar to Parkinson's disease (PD) (Horning *et al.*, 2015; Ou *et al.*, 2018). Furthermore, excessive exposure to Mn can also lead to disruptions of the respiratory and reproductive systems (Menezes-Filho *et al.*, 2009; dos Santos *et al.*, 2019).

The toxicity and adverse health effects of exposure to Mn-bearing PM depend on individual characteristics such as breathing rate, duration of exposure, and concentration, and the size of the particles (Lucchini, Martin and Doney, 2009; Morawska *et al.*, 2013; Kim, Kabir and Kabir, 2015). Furthermore, the solubility of the PM is an important factor for systematic uptake (Hernández-Pellón *et al.*, 2017). Symptoms of manganism include decreased memory, concentration, fatigue, headache, vertigo, loss of equilibrium, insomnia, tinnitus, trembling of fingers, muscle cramp, and rigidity (Menezes-Filho *et al.*, 2009; Haynes *et al.*, 2010).

Although such symptoms have been documented from occupational studies, environmental studies investigating exposure to airborne Mn-bearing particles have reported similar pre-clinical neurological effects (Lucchini *et al.*, 2007; Solís-Vivanco *et al.*, 2009; Carvalho *et al.*, 2018). Bowler *et al.* (2016) reported a correlation of long-term chronic environmental Mn exposure with impairment in motor function. The study found a change in postural and bilaterality in tremors which are more frequent in manganism (Bowler *et al.*, 2016). The chronic health outcomes are due to a cumulative exposure effect relationship (Squizzato *et al.*, 2018). However, the studies were using epidemiological approaches, which lack exposure assessment data and do not provide information on the source(s) of emission (Yue *et al.*, 2008).

### 1.2.5 Studies investigating Mn-bearing $PM_{2.5}$ in residential areas

Although Mn-bearing PM is ubiquitous in the atmosphere, anthropogenic sources such as ferromanganese smelters have been linked with low and high atmospheric concentrations of Mn-bearing PM in residential areas. Several studies have investigated Mn-bearing PM in

residential areas and the highest concentration levels were reported in residential areas near ferromanganese smelters (Otero-Pregigueiro *et al.*, 2018).

A study by Lucchini *et al.* (2007) measured atmospheric Mn in the respirable fraction in six areas two km from a manganese alloy plant in Brescia, Italy. The study reported a geometric mean of 0.69 µg $Mn/m^3$ and a range of 0.2–1.8 µg $Mn/m^3$. In the same study, Mn concentrations were 0.08 µg $Mn/m^3$ and ranged between 0.05–0.3 50 km downwind of the smelter (Lucchini *et al.*, 2007). Menezes-Filho *et al.* (2009) measured atmospheric Mn-bearing $PM_{2.5}$ in residential areas 1.3 km from a ferromanganese smelter plant in Salvador, Brazil. The authors reported atmospheric Mn concentrations ranging from 0.011–0.439 $\mu g/m^3$.

In another study conducted near a ferro and silico-manganese smelter in two Ohio towns, total suspended particles atmospheric Mn sampled from 2003–2013 were between 0.11–0.39 in Marietta and 0.17–1.5 in East Liverpool $\mu g/m^3$ (Colledge *et al.*, 2015). In a recent study conducted in two residential areas near a ferromanganese smelter in the north of Spain, Cantabria, Hernández-Pellón *et al.* (2017) highest daily atmospheric Mn concentrations were found to be 1 279 $ng/m^3$ and 2 062 $ng/m^3$

The findings from previous studies suggest that ferromanganese smelters are a major contributor to atmospheric Mn-bearing PM in residential areas (Parmalee and Aschner, 2016; Parsons-White and Spitzer, 2018). Furthermore, Mn-bearing PM can settle in nearby residential buildings and infrastructure and impact the indoor air quality (Weisel *et al.*, 2005; Pavilonis *et al.*, 2015; Urso *et al.*, 2015; Hänninen and Goodman, 2019). Moreover, it is stated that 35%–70% of indoor $PM_{2.5}$ is from the outdoor environment (Allen *et al.*, 2012; Lv *et al.*, 2017). The outdoor particles can enter indoor environments through infiltration, ventilation, or filtration mechanisms (Hasheminassab *et al.*, 2014; Koivisto *et al.*, 2019) and through openings and improperly sealed windows (Bowler *et al.*, 2016). $PM_{2.5}$ can also enter the indoor microenvironment through foot tracking (Lee *et al.*, 2002).

## 1.3 Problem statement

In South Africa, several studies (Myers *et al.*, 2003; Young, Myers and Thompson, 2005) assessing exposure to Mn-bearing PM have been conducted, however, they were focused and confined to occupational settings with little focus on incidental exposures at a community level. Davourie *et al.* (2017) stated that exposure to airborne Mn-bearing particles in occupational settings has been sufficiently investigated, however, non-

occupational exposure remains a significant concern (Davourie *et al.*, 2017). Furthermore, occupational exposure to Mn-bearing particles is characterised by intermittent high concentrations while environmental exposure consists of low concentrations for a prolonged period through multiple exposure routes (Rodríguez-Agudelo *et al.*, 2006; Solís-Vivanco *et al.*, 2009; Kornblith *et al.*, 2018).

Despite several gaps in understanding source to receptor relationship, only one study (Batterman *et al.*, 2011) in South Africa has investigated the physicochemical properties of airborne Mn-bearing PM and exposure thereof. Therefore, there is limited data regarding the physicochemical properties of PM and exposure assessment data in residential areas near ferromanganese smelters in South Africa (Hermanus, 2000). Subsequently, epidemiological studies (Wild, Bourgkard and Paris, 2009) use occupational data due to limited data (Niu *et al.*, 2010; Sly *et al.*, 2016). The limited data is attributed to the reluctance to conduct studies due to anticipated low concentration levels in residential areas near ferromanganese smelters (Sly *et al.*, 2016).

Such studies often use ambient concentration levels obtained from fixed monitoring stations that are located far from the receptor, and the study population is allocated to the same exposure (Turpin *et al.*, 2007; Hasheminassab *et al.*, 2014). Diapouli *et al.* (2011) and Gozzi *et al.* (2016) argued that the concentration of airborne PM obtained from fixed monitoring stations does not represent the exposure at the receptor level. The lack of exposure assessment data subsequently leads to poor development of pollution inventory and establishment of strategies or policies to improve air quality in residential areas in the industrialised parts of the country. Therefore, a study of this kind that intends to link the source and hazard is necessary to develop effective control measures to protect public health.

## 1.4 Justification

Source apportionment studies have been conducted in South Africa, however, the studies lacked information on the elemental composition of the PM (Galvão *et al.*, 2018). Consequently, limited emission inventories on industrial processes exist in the country since the implementation of an emission inventory depends on the correct determination of the elemental composition of PM (GroundWork, 2016). Therefore, to improve the emission inventory for source control or mitigation, the correct identification of the chemical signature remains an important variable that must be analysed (Ahmed, Guo and Zhao, 2017).

The objective of various source apportionment techniques is to determine emission sources and quantify their contribution (Li *et al.*, 2017). Determining the physicochemical properties of PM is important in understanding their origin, formation, and transformation mechanisms and the processes that can occur at their surface (Crenn *et al.*, 2018). Furthermore, to implement interventions that will be effective and efficient in protecting both public health and the environment, information on the main contributing source(s) is important (Aldabe *et al.*, 2011; Dong *et al.*, 2015; Hopke, 2016).

This study is relevant in that it builds on the main study titled "exposure to manganese in an African community", ethical clearance certificate (M150466). The main study aims to associate exposure to Mn-bearing PM and adverse health outcomes and is targeting adults over 40 years due to a higher prevalence of manganism in this age group. To achieve this, BGI PQ-100 samplers are used to collect samples at the three selected residential areas and human samples such as nails, saliva, and hair are collected from the participants. Furthermore, the participants are taken for an MRI scan to check for any presence of Mn particles in the brain. Pilot studies reported a significant prevalence of Parkinsonism (18%), anxiety, and depressive symptoms. Therefore, the MRI scan is done to validate the association between exposure to Mn-bearing PM and the identified health outcomes.

Questionnaires will also be administered to obtain information on the participant's residential and occupational history, potential confounders, mood, and behaviour changes. A series of tests will also be done using various measurement tools to assess the cognitive, memory, and motor function of the participants. The measurement tools include the matrix reasoning subtest from the Wechsler Abbreviated Scale of Intelligence, Object-Go-No-Go test, Letter Number Sequencing, Grooved Pegboard, and Unified Parkinson's Disease Rating Scale 3.

The main study has limitations, it lacks exposure assessments in the near field of the receptors. The main study will only use outdoor concentrations despite that people spend 70–90% of their time indoors where they are likely to be exposed. The current study will address the limitations by sampling indoor and outdoor $PM_{2.5}$ at the level of the receptor to reduce the uncertainty. The study further provides information on the morphology and elemental composition of the sampled $PM_{2.5}$.

Results from this study may help identify the emission source(s), pathway, and transport media of the particles, which are important for source apportionment. The results will also provide insight into the morphology, chemical composition, and identity of particles that the Meyerton residents are potentially exposed to. Therefore, the findings from the study can be

used to strengthen epidemiological data sets in the main study and other future studies. Moreover, the characterisation of PM is fundamental in identifying the emitting source(s) and implementing effective interventions to prevent exposure. Findings from this study will also be useful in policy formulation and decision making, particularly during town planning and the development of industrial and residential areas.

### 1.5 Hypothesis

This study hypothesised that the Mn-bearing $PM_{2.5}$ concentration will be higher outdoor relative to indoor in the three selected residential areas near the ferromanganese smelter in Meyerton.

### 1.6 Study Aim

To systematically characterise the similarities between indoor and outdoor $PM_{2.5}$ in three residential areas near the ferromanganese smelter in Meyerton.

### 1.7 Objectives

To achieve the above aims the following objectives were set out:

1. To determine indoor and outdoor mass concentration of the sampled $PM_{2.5}$ in the three selected residential areas near the ferromanganese smelter in Meyerton;
2. To compare the indoor and outdoor mass concentration of the sampled $PM_{2.5}$ in the three selected residential areas near the ferromanganese smelter in Meyerton;
3. To determine the physical properties of the sampled indoor and outdoor $PM_{2.5}$ in the three selected residential areas near the ferromanganese smelter in Meyerton.
4. To determine the elemental composition of the sampled indoor and outdoor $PM_{2.5}$ in the three selected residential areas near the ferromanganese smelter in Meyerton.

# CHAPTER 2: RESEARCH DESIGN AND METHODOLOGY

This chapter begins with a comprehensive description of the study area and the characterisation of the study parameters. A brief history of the ferromanganese smelter and products produced is given. The methods and materials used in the preparation of filters, sampling of particulate matter, and calculation of indoor and outdoor $PM_{2.5}$ mass concentration are outlined. The data analysis and statistical analysis used to determine the

I/O ratio and difference between indoor and outdoor $PM_{2.5}$ mass concentration are described. The chapter further describes the SEM-EDX used for studying the particle morphology and software used to convert particle size to particle number concentration of indoor and outdoor $PM_{2.5}$. The chapter ends by describing the ICP-MS used to study the elemental composition of the sampled indoor and outdoor $PM_{2.5}$.

## 2.1 Research design

This is a cross-sectional study that used a quantitative approach whereby we aimed to compare the physicochemical properties of indoor and outdoor Mn-bearing $PM_{2.5}$

## 2.2 Methods and materials

### 2.2.1 Description of the study area

The study was conducted in Meyerton which is located 15 kilometres north of Vereeniging, Gauteng Province with a global positioning system (GPS) coordinates 26.5854° S and 28.0069° E. Meyerton is under the Midvaal Municipality administration. The Midvaal is well known for its agricultural activities and it is surrounded by maize and dairy farmlands that supply most parts of Gauteng Province.

Meyerton has an area of 180.24 km² and a population size of 55 283 people consisting of 28 041 (50.72%) males and 27 242 (49.28%) females (Statistics South Africa, 2011). The area has an average temperature of 17 ºC, average rainfall of 34.4 mm, humidity 61%, and wind speeds of 6km/h. Approximately 22.7% of the population is between the ages of 0–14, 70% is between 15–64 and 7% is 65 years and above (Statistics South Africa, 2011). Approximately 77.5% of the households in Meyerton are formal dwellings while the remaining are informal settlements made mainly of corrugated iron and boards (Statistics South Africa, 2011).

Within Meyerton, three residential areas (Old Sicelo, New Sicelo, and Noldick) are located near and downwind of a ferromanganese smelter (Figure 1). Although these residential areas are in the same region, they have different characteristics and are at a different distance from the ferromanganese smelter. New Sicelo and Noldick are located near the smelter while Old Sicelo is located farther. Old and New Sicelo are the most densely populated residential areas relative to Noldick. Most of the dwellings in Noldick are constructed of cement blocks and they have ceilings. Most dwellings at New and Old Sicelo are predominantly shacks

constructed from corrugated Fe and boards. Such dwellings are naturally ventilated, thus allowing the outdoor PM to enter indoor environments through openings and cracks.

Most of the Noldick area is vegetated and paved relative to Old and New Sicelo, however, Old Sicelo has tree plantations compared to New Sicelo and Noldick. It has been proven that trees can help reduce the concentration of airborne particles through deposition (Xing and Brimblecombe, 2019). The lack of paving, vegetation, and tree plantations can influence the re-suspension of deposited dust during strong winds or other human activities. Old and New Sicelo are located west of the R59 which is one of Gauteng province's busiest freeways that connects to other neighbouring Provinces. The R551 and M61 roads pass through Noldick and New Sicelo and connect to neighbouring residential areas.

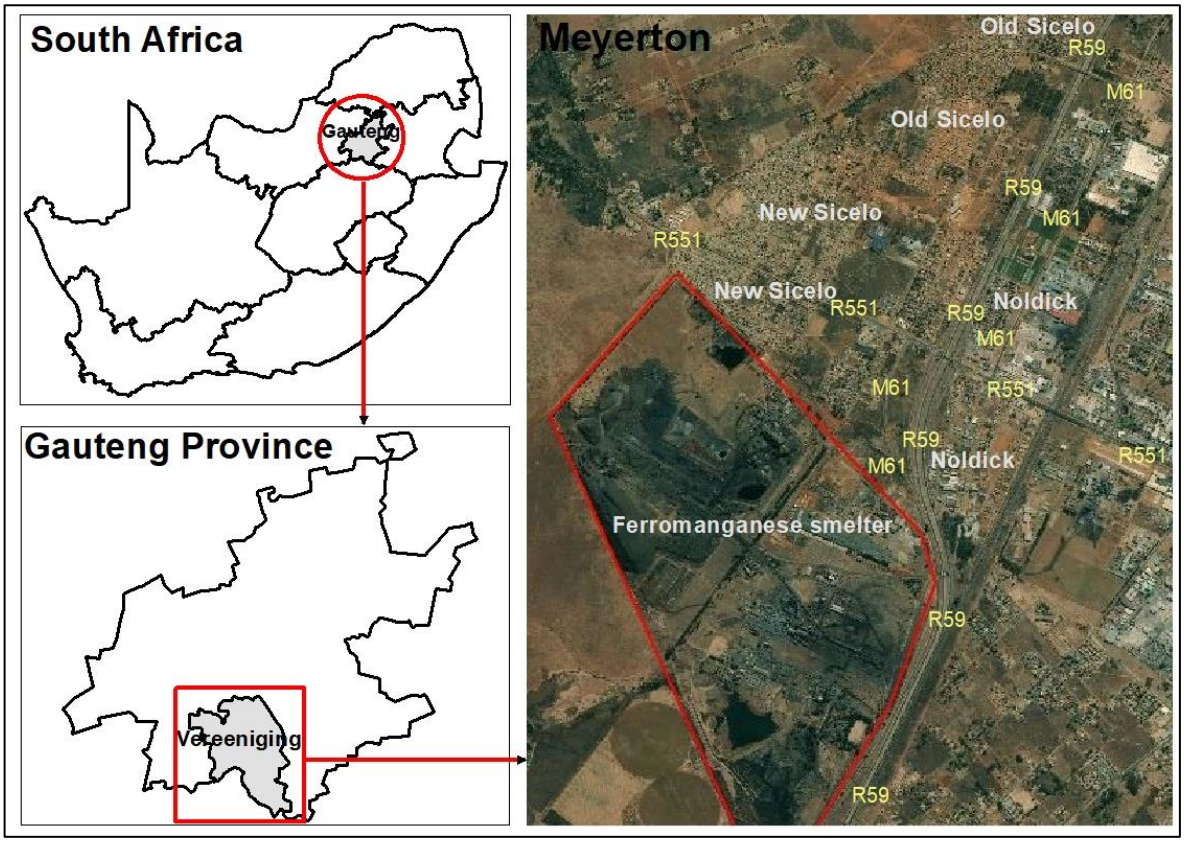


**Figure 1:** A geographical map of the study area (created Arcmap GIS and Google map)

The ferromanganese smelter was founded in 1939 by the late Dr. H.J van der Bijl who was a pioneer in the exploitation of minerals (Steenkamp and Basson, 2013). The smelter was initially built in the city of Vereeniging and named African Metals Cooperation Limited (Amcor) and produced HCFeMn and ferrosilicon (FeSi) using a three mega volt-ampere (MVA) furnace (Steenkamp and Basson, 2013). The production was expanded, and the company produced high-ferrochromium (HCFeCr), ferrotitanium (FeTi), medium

ferrochromium (MCFeCr), low ferrochromium (LCFeCr), ferrotungsten (FeW), Pb, and various types of stainless steel (Steenkamp and Basson, 2013).

In 1951, the Amcor smelter plant was renamed Samancor Manganese's Metalloys plant upon its relocation to Meyerton where it operates to date, however, the smelter has changed ownership from various companies in the past decades. The smelter is currently under the ownership of South32 which holds 60% of the shares while the remaining 40% is owned by Anglo American and it is called the South32 Metalloys alloy smelter. In 2012, Metalloys alloy ceased the production of SiMn and replaced it with HCFeMn (Steenkamp and Basson, 2013).

The Mn ore used by Metalloys alloy smelter is mined and transported from the Kalahari in the Northern Cape Province (Steenkamp and Basson, 2013). The Metalloys alloy smelter is one of the largest Mn smelters globally and produces HCFeMn (Creamer, 2013). In 2013, the Metalloys alloy smelter was installed with the biggest and distinctive furnace which would enable the company to beneficiate 30% of the Mn ore they produced locally (Creamer, 2013). The 81 MVA furnace can produce 120 000 tonnes of HCFeMn per year (Creamer, 2013). According to Creamer (2013), the production of MCFeMn and HCFeMn is approximately 60 and 480 kilotons annually, respectively. Steyn (2018), stated that the smelter can process more than one million tonnes of product annually.

### 2.2.2 Preparation of filters

Polycarbonate membrane (PCTE) filters (Zefon, Ocala, FL, USA) of 37 mm in diameter and pore size of 0.08 µm were conditioned in a controlled laboratory environment over 24 hours and pre-weighed gravimetrically in the occupational health laboratory at the University of the Witwatersrand. The weighing was done under ideal conditions (@ 21 ± 1˚C temperature and 35 ± 2% humidity) using a model CPA225D electronic microbalance scale (Sartorius, AG, Göttingen, Germany) that has a minimum resolution of 0.001 mg. The microbalance scale was calibrated internally by pressing the CAL button before weighing the filters. Before sampling, the filters were stored in a controlled laboratory environment with the temperature recorded at 22˚C and humidity 35%. Before and after sampling each filter was weighed three times and the average mass was used.

### 2.2.3 Sampling of indoor and outdoor $PM_{2.5}$

Sampling is a critical phase that can determine the success or failure of the experimental work, therefore the sampling equipment must be chosen carefully to achieve reliable results

(Galvão *et al.*, 2018). The sampling of airborne PM has been conventionally done using active samplers and the most used method of active sampling is by passing air through a filtering media using a pump (Elmes and Gasparon, 2017).

The active sampling technique ensures enough accumulation of PM on the filter for a statistically robust determination of the mass concentration thus providing reliable quantitative data (Elmes and Gasparon, 2017). It further allows accurate measurement of the air pumped through the filter so that the mass concentration can be calculated and reported as mass per cubic metre of air (Elmes and Gasparon, 2017).

The correct selection of a filter medium is critical to avoid misleading results, PCTE filters are suitable for microscopic analyses because they have a smooth surface area which makes it easier to detect single particles (Yue *et al.*, 2006; Genga *et al.*, 2018). PCTE filters are recommended for elemental analysis due to their low blank levels, inertness to gas adsorption, comprise of low impurities, low moisture absorption, high PM collection efficiency and they can withstand severe weather conditions (Izhar *et al.*, 2016; Genga *et al.*, 2018).

In this study, indoor and outdoor $PM_{2.5}$ was sampled concurrently using two identical Gilian GilAir 300plus pumps (Sensidyne, St Petersburg FL, USA) (Stanislawska *et al.*, 2017), connected to a Teflon tube that joins the pump and a 37 mm cassette (SKC Inc., Eighty-Four, PA, USA) fitted with a PCTE filter. The cassette was coupled with a 37 mm $PM_{2.5}$ Gs-3 multiple-inlet cyclone (SKC Inc., Eighty-Four, PA, USA) that separated the coarse and fine particles using centrifugal force (Boudissa *et al.*, 2006; Panda and Shiva Nagendra, 2018).

One pump was used to sample the outdoor $PM_{2.5}$ while the other pump was used to sample indoor $PM_{2.5}$ in the main activity room. Both pumps were placed indoors for security purposes and to protect the pumps from harsh environmental conditions such as rain and direct sunlight which can damage the pumps and affect their functionality. The samples were collected at a height of ~1.5 m, ~1 m away from walls, and ~1.2 m away from windows, doors, and ventilation inlets (Hoek *et al.*, 2008). Although the pumps are fitted with a battery with a life span of eight hours, they were connected to an electric charger as a backup. The pumps were continuously monitored to ensure that they are sampling effectively.

The airborne $PM_{2.5}$ was sampled at a constant flow rate of 2.75 L/min and the particles were deposited on the PCTE filters (Boudissa *et al.*, 2006) and the flow rate was checked before and after sampling using a Gilibrator (Sensidyne, St Petersburg FL, USA) for quality control.

The pumps provided the relapsed time in minutes and calculated the volume of air sampled. However, the volume was in litres per minute (L/min). Therefore, the volume was divided by a thousand to convert it into cubic metres ($m^3$).

Households sampled were those of participants that went the MRI scan as part of the main study. The houses were selected as part of the main study by drawing grids on the map of each residential area and two houses were selected from the grid. Thirty households were selected for the study and households sampled are those of the participants under the MRI scan for the main study.

Sampling was conducted from August to November 2019 and 60 samples consisting of 30 outdoor and 30 indoor $PM_{2.5}$ samples were collected. Indoor and outdoor $PM_{2.5}$ samples were collected concurrently at each household for ~24 hours and seven days a week. The 30 outdoor $PM_{2.5}$ samples comprised ten Old Sicelo, ten New Sicelo, and ten Noldick samples. Similarly, the 30 indoor samples comprised 10 Old Sicelo, 10, New Sicelo, and 10 Noldick $PM_{2.5}$ samples as shown in Table 1.

**Table 1:** Duration of the sampling campaigns and the number of houses sampled per residential area

| Sampling campaign | Sampling period | | Residential area | | |
|---|---|---|---|---|---|
| | Start | End | Old Sicelo | New Sicelo | Noldick |
| Campaign 1 | 06 September | 13 September | 1 | 2 | - |
| Campaign 2 | 13 September | 20 September | 1 | 1 | - |
| Campaign 3 | 20 September | 27 September | 1 | 2 | - |
| Campaign 4 | 27 September | 04 October | 1 | 1 | - |
| Campaign 5 | 04 October | 11 October | - | 1 | 1 |
| Campaign 6 | 11 October | 18 October | - | 2 | 1 |
| Campaign 7 | 25 October | 11 November | 2 | - | 2 |
| Campaign 8 | 01 November | 08 November | 1 | - | 2 |
| Campaign 9 | 08 November | 15 November | 2 | - | 2 |
| Campaign 10 | 16 November | 21 November | 1 | 1 | 2 |
| **Total sampled houses** | | | **10** | **10** | **10** |

### 2.2.4 Preparation of samples and analyses using scanning electron microscopy and energy-dispersive X-ray (SEM-EDX)

Electron microscopy techniques have been applied in several studies to characterise atmospheric particles for the past decades (Sielicki *et al.*, 2011; Riffault *et al.*, 2015). Relative to light microscopy, electron microscopes use a particle beam of electrons instead of visible light to illuminate the specimen and produce a magnified image (Ul-Hamid, 2018;

Kwiecińska, Pusz and Valentine, 2019). Electron microscopy can achieve resolutions of 0.05 nm and magnifications of up to 10 000 000× (Ul-Hamid, 2018; Kwiecińska, Pusz and Valentine, 2019). SEM creates magnified images thus providing microscopic information on the morphological properties of a sample (Zanetti-Ramos *et al.*, 2010).

SEM allows a focused electron beam to be scanned across the sample while under vacuum and collects the response of reflected electrons and photons to generate an image (Casuccio *et al.*, 2004; Kwiecińska, Pusz and Valentine, 2019). The ability of SEM to provide detailed information on the morphological and chemical properties of individual particles has made it the first choice method for identifying emitting sources affecting atmospheric air quality (Casuccio *et al.*, 2004; Li *et al.*, 2010).

During the analysis process, the specimens are exposed in SEM to the high-energy electron beam and provide information about the topography, morphology, and elemental composition (Brodusch, Demers and Gauvin, 2018). SEM is more helpful when characterising the morphological and elemental properties of single particles. (Moreno *et al.*, 2011). Therefore, SEM is a useful technique for distinguishing the origin of different particles based on their elemental composition and morphological properties (Satsangi and Yadav, 2014; Ul-Hamid, 2018).

The interaction of the electron beam with the sample produces various signals that can be monitored with suitable detectors (Casuccio *et al.*, 2004). The SEM analyses include the secondary electrons (SE), back-scattered electrons (BSE), Auger electrons and X-rays, and photons of different energies (Sielicki *et al.*, 2011; Ellingham, Thompson and Islam, 2018). However, SE and BSE are more significant and commonly used (Ul-Hamid, 2018). The SE yields an image with a three-dimensional view and a high-depth field while the BSE yields an image containing compositional information since the signal depends on the atomic number of the particle examined (Casuccio *et al.*, 2004).

In this study, the size and morphological properties of two indoor and two outdoor $PM_{2.5}$ samples were analysed using a Tescan Vega3 LMH SEM (Tescan, Brno, Czech Republic) at the University of Johannesburg (Stanislawska *et al.*, 2017). SEM was coupled with X-max 50 $mm^2$ energy-dispersive X-ray spectroscopy (EDX) (Oxford Instruments, Abingdon, Oxfordshire, UK) which was used for mapping and analysing the elemental composition of the $PM_{2.5}$. The EDX has a detection limit of 0.1 weight percent (Wt%).

EDX is the most commonly used X-ray detector in the SEM for analysing elements in high concentrations (Carvalho, 2018; Ul-Hamid, 2018). The interaction of the electron beam with the sample being analysed results in the emission of X-rays and specific elements are separated into an energy spectrum by the EDX detector (Ellingham, Thompson and Islam, 2018). The energy and intensity of the X-rays emitted by the sample were processed and recorded as a spectrum (Casuccio *et al.*, 2004).

Approximately 1 $cm^2$ was cut from the centre of each of the selected PCTE filters containing the sampled PM using a pair of scissors and mounted onto an Al stub using a double-sided adherent carbon conductive tape (Labrada-Delgado *et al.*, 2012). The mounting allows the determination of the morphology, surface structure, and elemental composition of the particles. Non-conductive samples must be coated and it is a common practice to coat all non-carbon content samples, the coating enhances the contrast of the SEM images and reduces the electrostatic charging of particles (Labrada-Delgado *et al.*, 2012; Ul-Hamid, 2018). The PCTE filters are non-conductive, therefore, the samples were sputter-coated with a thin layer of carbon (<10 nm) using an Agar Turbo Carbon coater (Agar Scientific, Stansted, UK).

After coating, the stubs containing the carbon-coated samples were loaded into an SEM-EDX vacuum chamber for analyses. The particle morphology was analysed using the back-scattered electron detector at a 20 kV accelerating voltage, using an electron beam intensity of ~3 nA at a working distance of 15 mm from the detector (Pallarés *et al.*, 2020). Using 20 kV improves imaging of the surface and internal structure of the particles relative to lower accelerating voltages (Ul-Hamid, 2018). All the particles analysed in the field of view were photographed, the output images were acquired with 1024 × 768 pixels and 256 greyscale levels.

Similar to Kutchko and Kim (2006), the elemental composition was analysed in a spot mode where the beam was localised on a single area that was manually chosen within the viewed sample, with the EDX focused at 15 mm. The different peaks were identified and the oxford software Aztec (version 3.3 SPI) was used to obtain the peak intensities. However, EDX is not without limitations. The results from the EDX are semi-quantitative and EDX tends to be inaccurate, particularly if the concentration of elements in the sample is low (Li *et al.*, 2017). Nonetheless, Kutchko and Kim (2006) stated that conclusions can be made from the semi-quantitative information from EDX.

SEM-EDX has its strengths and limitations, there is scientific evidence suggesting that the samples observed under SEM are susceptible to mass loss of adsorbed water or volatiles due to the vacuum operation (Khan, Oh and Kim, 2020). Furthermore, there is a possibility of damage by electron beam heating or electrostatic disruption (McDonald and Biswas, 2004). The quality of the images depends on the input parameters determined by the operator (Ul-Hamid, 2018). Elements in small concentrations are unlikely not to be detected because the resolution of the EDX is approximately 0.5% (Carvalho, 2018).

### 2.2.5 Preparation of samples and analyses using inductively coupled plasma mass spectrometry (ICP-MS)

Inductively coupled plasma-mass spectroscopy plays a vital role in research, thus it has become the preferred method for elemental analysis (Ammann, 2007). Elemental analysis is commonly done to understand the overall spectrum of the elements contained within the PM (Pröfrock and Prange, 2012; Gross, 2017). Such information can be useful for tracing the source(s) of the PM and to determine the harmful human health effects (Galvão *et al.*, 2018). Literature indicates that ICP-MS is a widely used technique for the elemental analysis of PM and the number of studies using this technique has increased by two folds in the past decades (Galvão *et al.*, 2018).

Similarly, in this study, ICP-MS was used to determine the elemental composition of indoor and outdoor $PM_{2.5}$ to trace the emitting source. Three indoor and outdoor samples were analysed at the University of Johannesburg Spectrum Laboratory, Auckland Park campus using a Perkin Elmer NexION 300 ICP-MS (Perkin Elmer, Waltham, MA, USA). The sample filters were folded and placed inside pre-cleaned microwave digestion vessels. A 9 mL supra pure (Merc) nitric acid ($HNO_3$), and 1 mL supra pure (Merc) hydrogen peroxide ($H_2O_2$) was added to each vessel. A reagent blank was included with the batch as a control. The vessels were closed and placed in a Mars 6 microwave (Zhang *et al.*, 2019).

The samples were then transferred to a 50 mL volumetric flask and made up to the mark using 18.2 MΩ/cm$^2$ ultrapure water. Calibration standards of 0 µg/L, 0.1 µg/L, 0.5 µg/L, 1.0 µg/L, 5.0 µg/L and 10 ug/L were prepared from 100 mg/L NIST traceable stock standards (Masekameni *et al.*, 2020). The samples were then filtered using a 0.45 µm syringe filter and diluted ten times (1 mL diluted to 10 mL) before analysis. ICP-MS technique and procedure were conducted for the blank filter (Masekameni *et al.*, 2020). The elements analysed using the ICP-MS included Mn, Magnesium (Mg), Silicon (Si), (Lead) Pb, Vanadium (V),

Cadmium (Cd), Sodium (Na), Iron (Fe), Cobalt (Co), Nickel (Ni), Copper (Cu), Chromium (Cr), and Zinc (Zn).

## 2.3 Data analysis

### 2.3.1 Indoor and outdoor $PM_{2.5}$ mass concentration

The gravimetric weighing was done to get the post mass of the filter using the same electronic microbalance (model-CPA225D, Sartorius, AG, Göttingen, Germany). To obtain the mass of $PM_{2.5}$. Each filter was weighed three times and the average mass was used. The final corrected mass was calculated using equation (1).

$$Final\ mass = field\ filter(post - pre) + (post - pre)blank\ filter \quad (1)$$

Where the field filter post mass is the mass collected on the filter after sampling, the field pre-mass is the mass recorded in the laboratory before sampling. The field blank post and pre are the mass recorded after transportation and before transportation of filters, respectively. The mass concentration was calculated using equation (2).

$$Concentration = \frac{m}{v} \quad (2)$$

Where (m) is the final mass calculated using equation 1, and (v) is the volume obtained by dividing the volume of sampled air provided by the pump by a thousand. The atmospheric mass concentration of particles is commonly measured in nanogram (ng/m³), microgram (µg/m³), gram (g/m³), or milligram (mg/m³) per cubic metre (Moreno *et al.*, 2011). In this study, the mass concentration was reported in µg/m³.

The I/O ratio was calculated to determine the difference between the indoor and outdoor mass concentration and to determine if there is any contribution of the outdoor PM to the indoor environment. The I/O ratio was obtained using equation (3).

$$C_i = \frac{C_{in}}{C_{out}} \quad (3)$$

Where $C_i$ is the indoor-outdoor ratio, $C_{in}$ is the indoor $PM_{2.5}$ mass concentration and $C_{out}$ is the outdoor $PM_{2.5}$ mass concentration.

### 2.3.2 Comparison of indoor and outdoor $PM_{2.5}$ mass concentrations

Indoor and outdoor $PM_{2.5}$ mass concentrations were compared statistically using an F-test and a Student t-test. The data were entered into a Microsoft Excel 2019 spreadsheet (Redmond, Washington, USA) and the F-test was first used to determine if there is an equal or unequal variance between the standard deviation between and outdoor $PM_{2.5}$ concentrations. The null hypothesis for the F-test was that there is an equal variance between the standard deviations of indoor and outdoor $PM_{2.5}$ concentrations. The alternate hypothesis was that there was an unequal variance between the standard deviation of indoor and outdoor $PM_{2.5}$ concentrations.

The F-test also helped determine the type of t-test to employ (i.e. t-test (i): two samples assuming equal variances or t-test (ii): two samples assuming unequal variances) (Chen *et al.*, 2018). A *p*-value equal to or less than 0.05 indicated a significant difference and the null hypothesis was rejected. A *p*-value greater than 0.05 indicated a non-significant difference and the null hypothesis was accepted.

A Student t-test was based on the outcome of the F-test. The Student t-test was used to check for a statistically significant difference between the means of the indoor and outdoor $PM_{2.5}$ mass concentrations. The Student t-test was performed at a 95% confidence level and a *p*-value greater than 0.05 indicated a non-statistically significant difference while a *p*-value equal to or less than 0.05 indicated a statistically significant difference (Figueiredo Filho *et al.*, 2013).

### 2.3.3 Scanning electron microscopy and energy-dispersive X-ray (SEM-EDX)

The size of the particles was determined using version 1.46r of ImageJ (NIH, Maryland, USA), an open-source software. The representative indoor and outdoor SEM images were loaded on the ImageJ software which counted the number of particles and their sizes automatically. The SEM images were threshold before analysis to obtain the best results. The ImageJ software has been used in several studies (Satsangi and Yadav, 2014; Stebounova *et al.*, 2018; Makonese, Meyer and von Solms, 2019) to determine the number and size distribution of particles.

### 2.3.4 Inductively coupled plasma mass spectrometry (ICP-MS)

Indoor and outdoor concentrations of the elements distributed on the sampled $PM_{2.5}$ were calculated using equation (4) (Arı, Arı and Gaga, 2020).

$$C_{element} = \frac{M_e - field\ blank}{V} \quad (4)$$

Where ($C_e$) is the concentration of the element in µg, ($M_e$) is the mass of the element from the ICP-MS, and (V) is the volume in cubic metres ($m^3$).

### 2.4 Quality control

All the standard operating procedures were followed when weighing, transporting, and connecting the equipment to prevent the risk of interference that can lead to errors. Standard pendulums weighing 100 and 200 g were weighed on the microbalance before and after sampling to calibrate the scale and to validate the results. All the filters were prepared in a dust-free laboratory with controlled conditions. Forceps were used to load and unload the filters while wearing dust-free surgical gloves to avoid cross-contamination. Each filter was weighed three times before and after sampling and the average mass was used.

A blank filter was prepared for each sampling campaign and it was transported with the filed filters, the blank filter was also placed next to the sampling field filters. The blank filters were used to account for any change in any moisture content due to environmental conditions and to account for cross-contamination during transportation. One blank filter was analysed using SEM-EDX for morphology and elemental composition to ensure that the filters were not contaminated and to get the background of the filters and another was analysed using ICP-MS to check if the filter was not contaminated. The mass concentration of the elements on the blanks was subtracted from the field filters used to sample the $PM_{2.5}$.

The flow rate of the pump was checked before and after sampling using a rotameter. The flow rate was also verified using a bubble flow metre Gilibrator (Sensidyne, St Petersburg FL, USA) for quality control and the fluctuation was within the 5% deviation.

# CHAPTER 3: RESULTS

This chapter begins with the descriptive results of indoor and outdoor $PM_{2.5}$ mass concentrations obtained using gravimetric techniques. $PM_{2.5}$ I/O ratios and inferential results between indoor and outdoor $PM_{2.5}$ mass concentrations are also presented. The chapter further provides results on the physical properties of indoor and outdoor $PM_{2.5}$ obtained using SEM and the semi-quantitative elemental composition of the $PM_{2.5}$ obtained using EDX. The chapter ends with the results on the elemental composition of indoor and outdoor $PM_{2.5}$ obtained using ICP-MS.

## 3.1 Indoor and outdoor $PM_{2.5}$ mass concentrations obtained gravimetrically

As shown in Table 2, it can be noted that outdoor $PM_{2.5}$ mass concentration was higher than indoor. The average indoor $PM_{2.5}$ mass concentration was 10.99 ± 5.10 µg/m$^3$ while the outdoor average concentration was 24.97 ± 6.77 µg/m$^3$. The I/O ratio was less than 1 suggesting that indoor $PM_{2.5}$ mass concentration was influenced by outdoor $PM_{2.5}$.

**Table 2**: Descriptive statistics for indoor and outdoor $PM_{2.5}$ mass concentrations (µg/m$^3$) levels and indoor-outdoor ratio in Meyerton

| | N | Min | Mean | Max | SD | Lower quartile | Upper quartile | I/O |
|---|---|---|---|---|---|---|---|---|
| **Indoor** | 30 | 2.88 | 10.99 | 19.19 | 5.10 | 9.08 | 12.89 | 0.44 |
| **Outdoor** | 30 | 11.68 | 24.97 | 40.44 | 6.77 | 22.44 | 27.49 | |

Min: minimum, Max: maximum, SD: standard deviation, I/O: indoor-outdoor ratio

In Figure 2, the variation between indoor and outdoor $PM_{2.5}$ mass concentrations for the three residential areas is shown. It can also be noted that outdoor $PM_{2.5}$ mass concentrations were higher than indoor. Old Sicelo presented the highest average indoor $PM_{2.5}$ mass concentration of 2.62 µg/m$^3$ while Noldick presented the highest average outdoor $PM_{2.5}$ mass concentration of 21.66 µg/m$^3$.

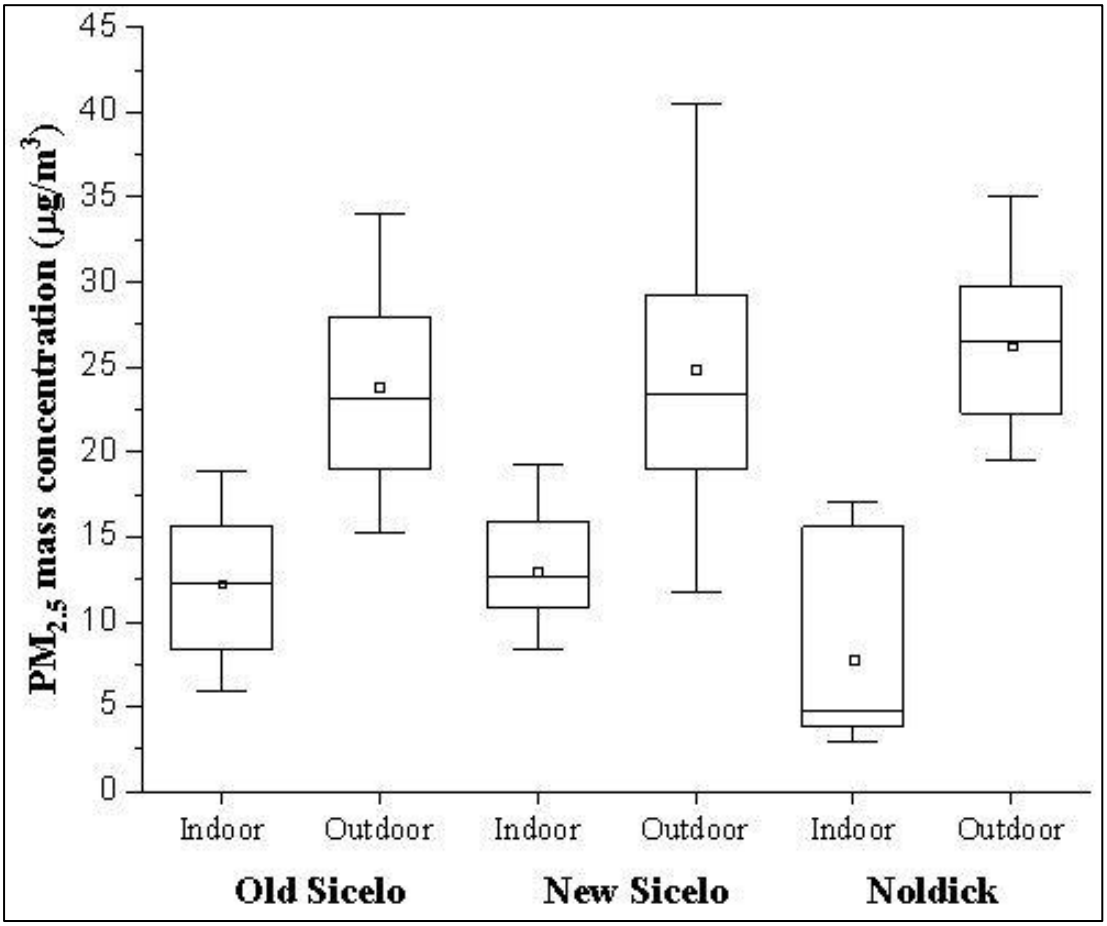


**Figure 2:** Box and whisker plots comparing indoor and outdoor $PM_{2.5}$ mass concentrations ($\mu g/m^3$) across the three residential areas

Table 3 shows a summary of the I/O ratios of the three residential areas. It can be noted that the average I/O ratios at Old Sicelo, New Sicelo, and Noldick were 0.50 ± 0.07, 0.54 ± 0.10, and 0.27 ± 0.17, respectively. Similar to the overall I/O ratio (Table 2), the I/O ratios across the three residential areas were less than 1, indicating that indoor $PM_{2.5}$ mass concentrations were less than the outdoor.

**Table 3:** Descriptive statistics of indoor-outdoor ratios across the three residential areas

| Parameter | Old Sicelo | New Sicelo | Noldick |
|---|---|---|---|
| **Minimum** | 0.39 | 0.39 | 0.14 |
| **Maximum** | 0.60 | 0.71 | 0.54 |
| **Mean** | 0.50 | 0.54 | 0.27 |
| **Standard deviation** | 0.07 | 0.10 | 0.17 |

### 3.2 Inferential statistics of indoor and outdoor $PM_{2.5}$ mass concentrations

Table 4 shows the inferential statistics for indoor and outdoor $PM_{2.5}$ mass concentrations in Meyerton. It can be noted that there was a significant percentage mean difference (55.99%)

between indoor and outdoor $PM_{2.5}$ mass concentrations. Furthermore, a statistically significant difference was found ($P$<0.05) between indoor and outdoor $PM_{2.5}$ mass concentrations.

**Table 4:** Statistical analysis of indoor and outdoor $PM_{2.5}$ mass concentration ($\mu g/m^3$) in Meyerton

| | N | Mean | % Difference | F-Value | P-Value | Sig @ 95% |
|---|---|---|---|---|---|---|
| **Indoor** | **30** | 24.97 | | | | |
| **vs** | | | 55.99 | 1.76 | $5.8\times10^{-13}$ | Yes |
| **Outdoor** | **30** | 10.99 | | | | |

sig@ 95%: statistically significant at 95% confidence interval

In Table 5, inferential statistics of indoor and outdoor $PM_{2.5}$ mass concentrations for the three residential areas are presented. Similarly, there was a significant percentage mean difference between indoor and outdoor $PM_{2.5}$ mass concentrations across the three residential areas. The mean percentage difference between indoor and outdoor $PM_{2.5}$ mass concentrations at Old Sicelo, New Sicelo, and Noldick were 48.51%, 48.02%, and 70.32%, respectively. A statistically significant difference was found ($P$<0.05) between indoor and outdoor $PM_{2.5}$ mass concentrations for the three pairings.

**Table 5:** Statistical analysis of indoor and outdoor $PM_{2.5}$ mass concentration ($\mu g/m^3$) across the three residential areas.

| Pairings | N | Mean | % Difference | F-Value | P-Value | Sig @ 95% |
|---|---|---|---|---|---|---|
| **Old Sicelo** | | | | | | |
| **Indoor** | 10 | 12.25 | | | | |
| **vs** | | | 48.51 | 2.02 | $6.5\times10^{-5}$ | Yes |
| **Outdoor** | 10 | 23.79 | | | | |
| **New Sicelo** | | | | | | |
| **Indoor** | 10 | 12.93 | | | | |
| **vs** | | | 48.02 | 7.49 | $1.2\times10^{-3}$ | Yes |
| **Outdoor** | 10 | 24.87 | | | | |
| **Noldick** | | | | | | |
| **Indoor** | 10 | 7.78 | | | | |
| **vs** | | | 70.32 | 1.47 | $3.7\times10^{-7}$ | Yes |
| **Outdoor** | 10 | 26.23 | | | | |

sig@ 95%: statistically significant at 95% confidence interval

### 3.3 Morphology of indoor and outdoor $PM_{2.5}$ obtained using SEM-EDX

In this section, the intention was to check the similarities in the morphology of indoor and outdoor $PM_{25}$. Figure 3, shows representative SEM images and EDX spectrum for the blank filter. It can be noted that no particles were detected implying that the filters were not

contaminated. The micro-structure shown in the images indicates the material used to construct the PCTE filters. Since no particles were detected, it implies that the filters were suitable for field use.

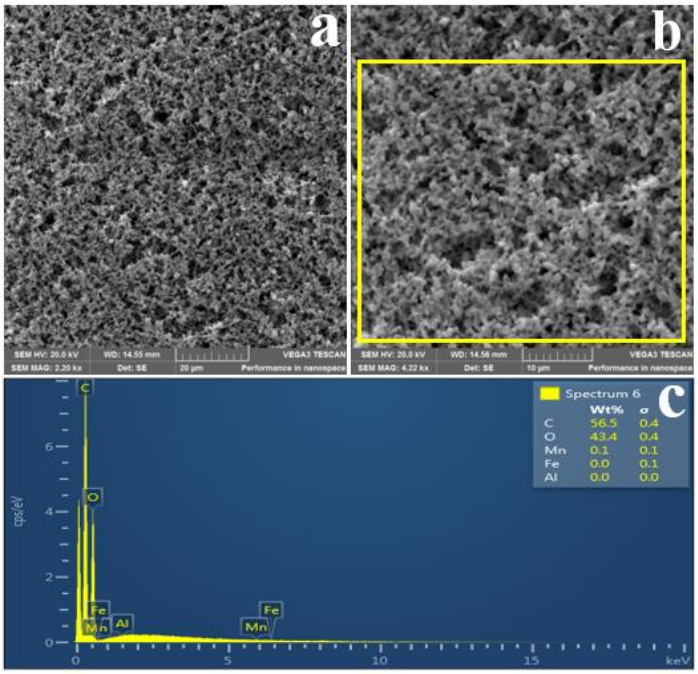


**Figure 3:** SEM images of the blank filter; (**a**) image captured at 20 µm (**b**) image captured at 10 µm, (**c**) EDX spectrum of the portion highlighted in yellow

As shown in Figure 4, indoor and outdoor representative SEM images of $PM_{2.5}$ sampled at Old Sicelo are shown together with the EDX spectrums. It can be noted that indoor $PM_{2.5}$ consisted of irregular and single spherical particles enriched with elements in decreasing order of Si > Al > Fe >S. It can also be noted that outdoor $PM_{2.5}$ consisted of irregular agglomerated particles enriched with Si > Al > Fe > Ca > S.

**Old Sicelo**

**Indoor** **Outdoor**

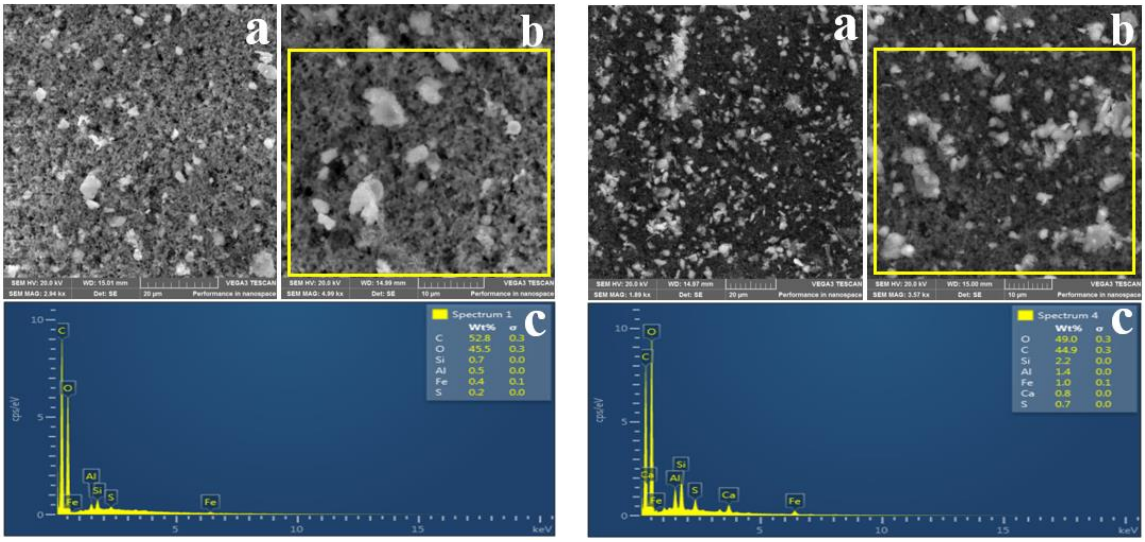


**Figure 4:** SEM images of indoor and outdoor $PM_{2.5}$ sampled at Old Sicelo; (**a**) image captured at 20 µm (**b**) image captured at 10 µm, (**c**) EDX spectrum of the portion highlighted in yellow

In Figure 5, indoor and outdoor representative SEM images of $PM_{2.5}$ sampled at New Sicelo are shown together with the EDX spectrums. It can be noted that indoor $PM_{2.5}$ consisted of irregular and single spherical particles enriched with Si > Al > Mn. It can also be noted that outdoor $PM_{2.5}$ consisted of irregular agglomerated particles enriched with Si > Al > Fe > Ca >S > Mn.

**New Sicelo**

**Indoor** **Outdoor**

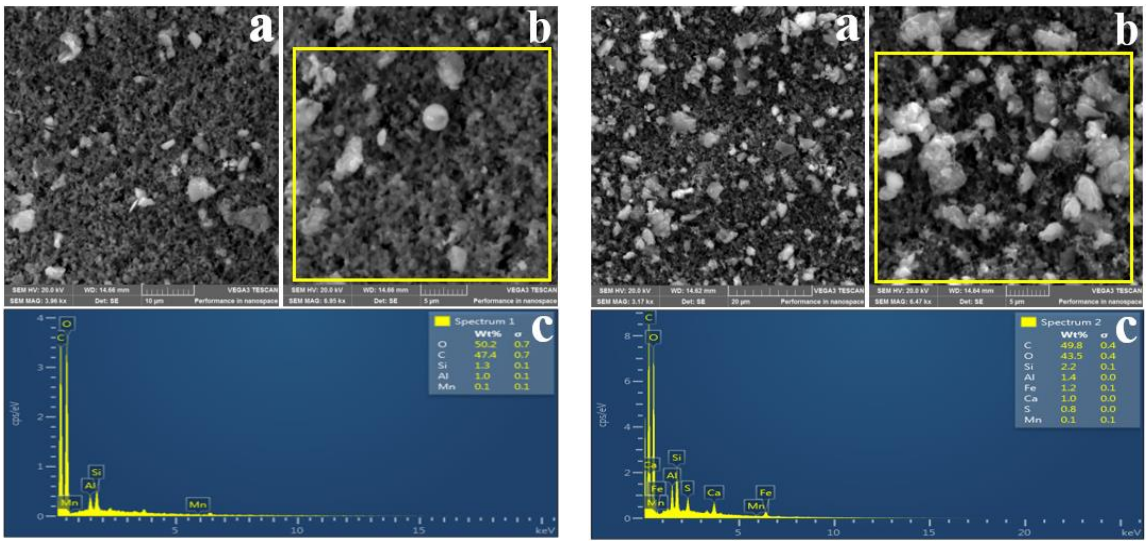


**Figure 5:** SEM images of indoor and outdoor $PM_{2.5}$ sampled at New Sicelo; ((**a)** indoor) image captured at 10 µm, ((**a)** outdoor) image captured at 20 µm (**b**) image captured at 5 µm, (**c**) EDX spectrum of the portion highlighted in yellow

In Figure 6, indoor and outdoor representative SEM images of $PM_{2.5}$ sampled at Noldick are shown together with the EDX spectrums. It can be noted that indoor $PM_{2.5}$ consisted of irregular particles enriched with Si > Al > Fe > Ca >S. It can also be noted that outdoor $PM_{2.5}$ consisted of irregular and agglomerated particles enriched with Si > Al > Fe > S > K> Ca >.

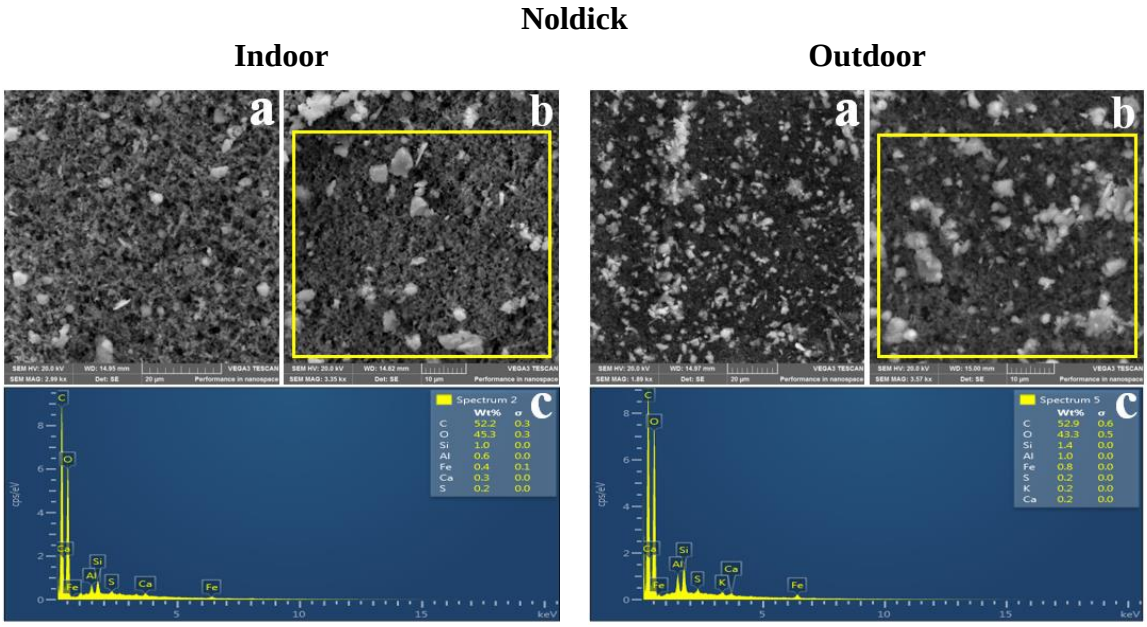


**Figure 6:** SEM images of indoor and outdoor $PM_{2.5}$ sampled at Noldick; (**a**) image captured at 20 µm (**b**) image captured at 10 µm, (**c**) EDX spectrum of the portion highlighted in yellow

Table 6, the elemental composition of indoor and outdoor $PM_{2.5}$ sampled across the three residential obtained using EDX is presented. Although most of the selected elements were not detected by the EDX, it can be noted that the outdoor $PM_{2.5}$ had the highest concentration of elements relative to indoor. The limit of detection for the EDX was 0.1 weight percent (Wt%).

**Table 6:** A summary of the elements (Wt%) detected using EDX

| elements | Old Sicelo | | New Sicelo | | Noldick | |
|---|---|---|---|---|---|---|
| | Indoor | Outdoor | Indoor | Outdoor | Indoor | Outdoor |
| **Mn** | <LoD | <LoD | 0.10 | 0.10 | <LoD | <LoD |
| **Al** | 0.50 | 1.40 | 1.00 | 1.40 | 0.60 | 1.00 |
| **Si** | 0.70 | 2.20 | 1.30 | 2.20 | 1.00 | 1.40 |
| **K** | <LoD | <LoD | <LoD | <LoD | <LoD | 0.20 |
| **Ca** | <LoD | 0.80 | <LoD | 1.00 | 0.30 | 0.20 |
| **Fe** | 0.40 | 1.00 | <LoD | 1.20 | 0.40 | 0.80 |
| **S** | 0.20 | 0.70 | <LoD | 0.80 | 0.20 | 0.20 |

<LoD: below limit of detection

In Figure 7, the size distributions of indoor and outdoor $PM_{2.5}$ across the three residential areas are shown. It can be noted that indoor particles ranged between 0.1–0.7 µm in diameter

and were dominated by particles of 0.1 µm. However, most particles were found in the 0.1 µm size bin. Outdoor particles ranged between a diameter of 0.1 and 1.3 µm and were also dominated by particles of 0.1 µm.

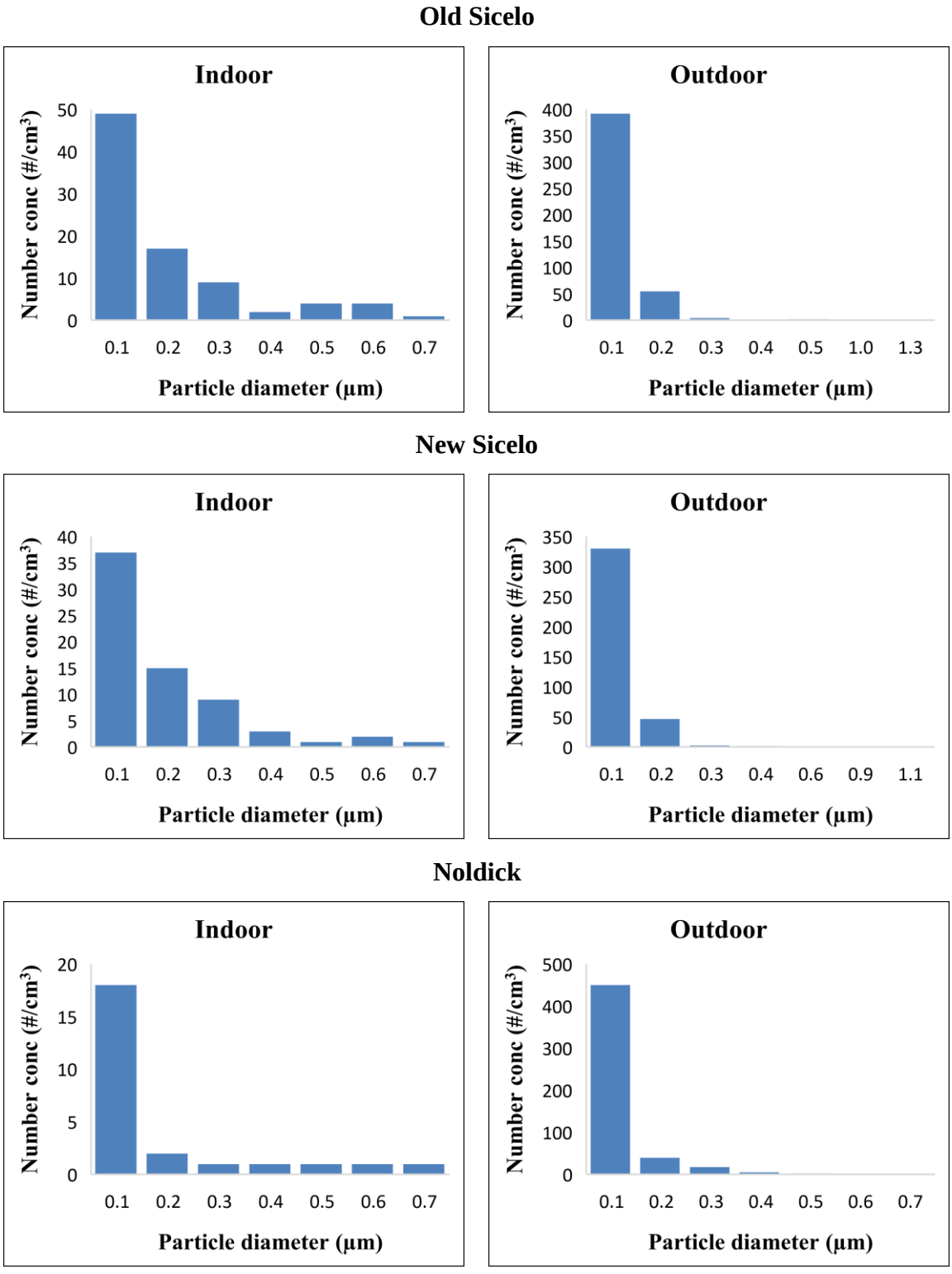


**Figure 7:** Size distribution of indoor and outdoor $PM_{2.5}$ sampled across the three residential areas

In Figure 8, the average concentrations of elements found on indoor and outdoor $PM_{2.5}$ in Meyerton are presented. It can be noted that outdoor elemental concentrations were higher than indoor. The highest average concentrations of elements were SI > Fe > Mn > Na > Mg > Zn. The average indoor and outdoor Mn concentrations were 1.30 µg/m$^3$ and 5.36 µg/m$^3$, respectively.

### 3.4 Elemental composition of indoor and outdoor $PM_{2.5}$ obtained using ICP-MS

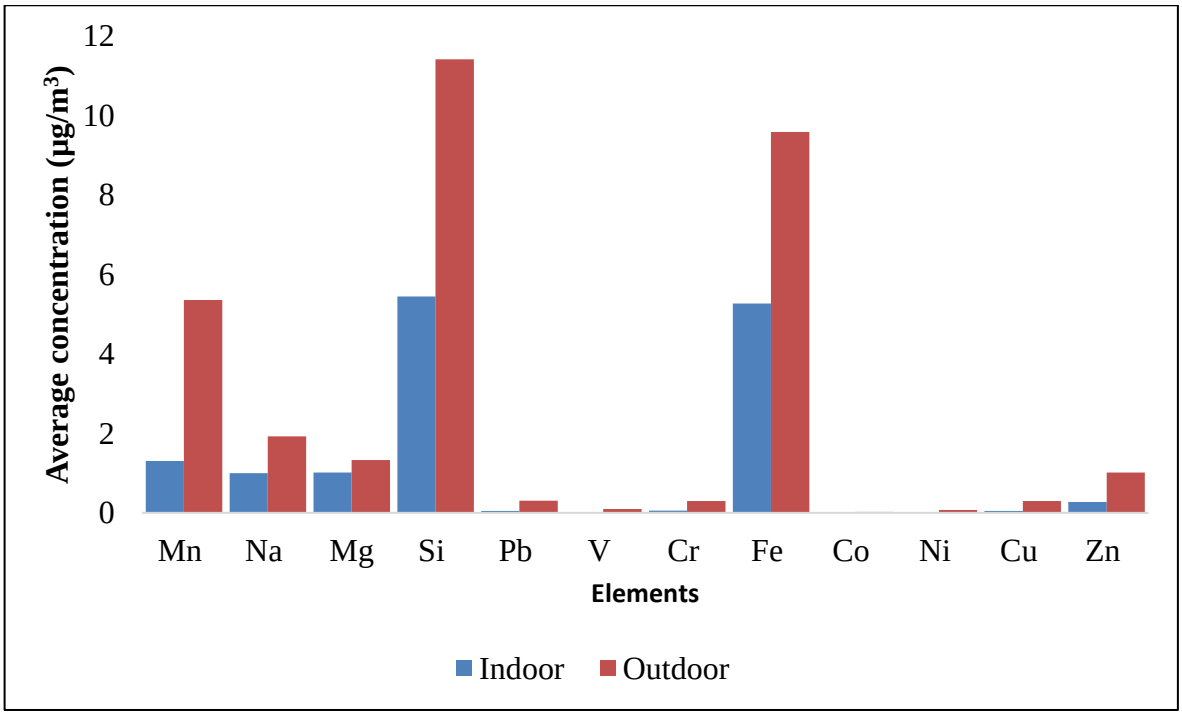


**Figure 8:** Average indoor and outdoor elemental concentrations (µg/m$^3$) distributed on the sampled $PM_{2.5}$ in Meyerton

In Table 7, the concentrations of elements found on indoor and outdoor $PM_{2.5}$ across the three residential areas are presented. It can be noted that outdoor concentrations of elements were higher than indoor. Noldick had the highest indoor and outdoor Mn concentrations. The limit of quantification for K and Cd were <10.67 and <0.033, respectively.

**Table 7:** Indoor and outdoor elemental concentration (µg/m$^3$) distributed on the sampled $PM_{2.5}$ across the three residential areas

| Elements | Old Sicelo | | New Sicelo | | Noldick | |
|---|---|---|---|---|---|---|
| | Indoor | Outdoor | Indoor | Outdoor | Indoor | Outdoor |
| **Mn** | 1.2045 | 3.9739 | 1.0346 | 5.5495 | 1.6712 | 6.5604 |
| **Na** | 0.9193 | 2.9715 | 1.1837 | 2.0935 | 0.8950 | 0.7115 |
| **Mg** | 1.5450 | 1.9122 | 0.6943 | 1.1227 | 0.8178 | 0.9574 |
| **Si** | 4.7417 | 11.3543 | 6.2718 | 15.3786 | 5.3376 | 7.5356 |
| **K** | <LoQ | <LoQ | <LoQ | <LoQ | <LoQ | <LoQ |
| **Pb** | 0.0258 | 0.2958 | 0.0656 | 0.1037 | 0.0494 | 0.5098 |

| | | | | | | |
|---|---|---|---|---|---|---|
| **V** | 0.0024 | 0.2045 | 0.0225 | 0.0268 | 0.0225 | 0.0544 |
| **Al** | <LoQ | <LoQ | <LoQ | <LoQ | <LoQ | <LoQ |
| **Cr** | 0.0586 | 0.3284 | 0.0540 | 0.0631 | 0.0610 | 0.5136 |
| **Fe** | 3.8665 | 10.5339 | 7.0881 | 12.0622 | 4.8544 | 6.1707 |
| **Co** | 0.0046 | 0.0667 | 0.0073 | 0.0091 | 0.0074 | 0.0080 |
| **Ni** | 0.0123 | 0.0882 | 0.0074 | 0.0510 | 0.0222 | 0.0800 |
| **Cd** | <LoQ | <LoQ | <LoQ | <LoQ | <LoQ | <LoQ |
| **Cu** | 0.0241 | 0.3270 | 0.0317 | 0.2742 | 0.0866 | 0.2819 |
| **Zn** | 0.1422 | 1.7705 | 0.3307 | 0.7567 | 0.3446 | 0.5178 |

<LoQ: below limit of quantification

In Figure 9, the contribution of the elements on the sampled indoor and outdoor $PM_{2.5}$ is presented in percentages. It can be noted that Si > Fe > Mn >Mg contributed most on indoor $PM_{2.5}$. It can also be noted that Si > Fe > Mn >Na contributed more to outdoor $PM_{2.5}$.

**Old Sicelo**

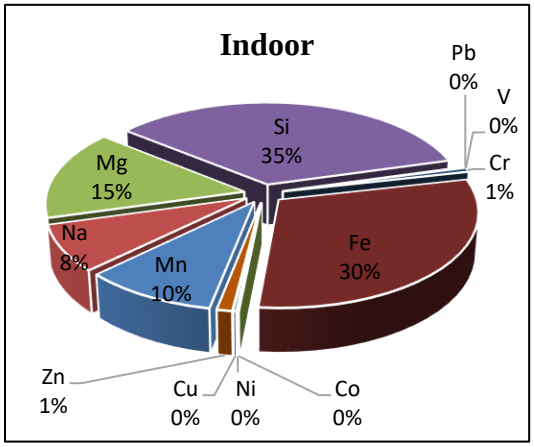


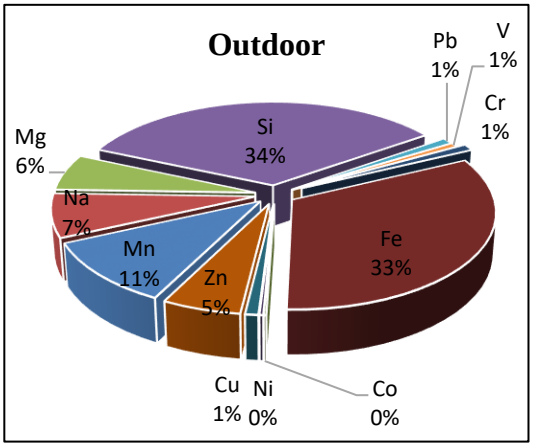


**New Sicelo**

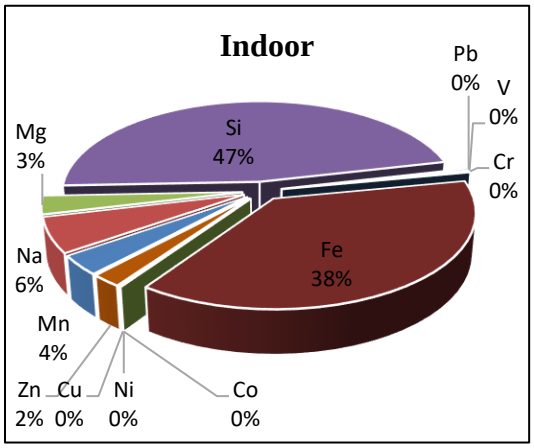


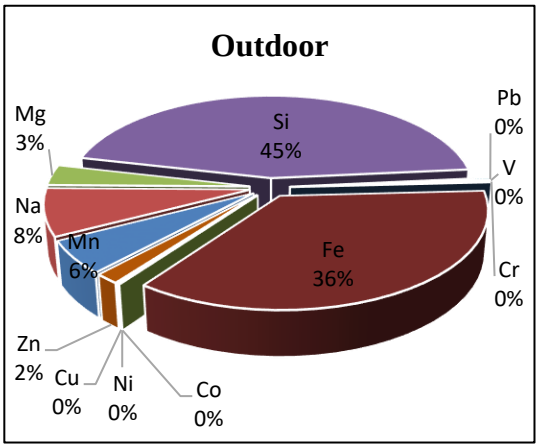


**Noldick**

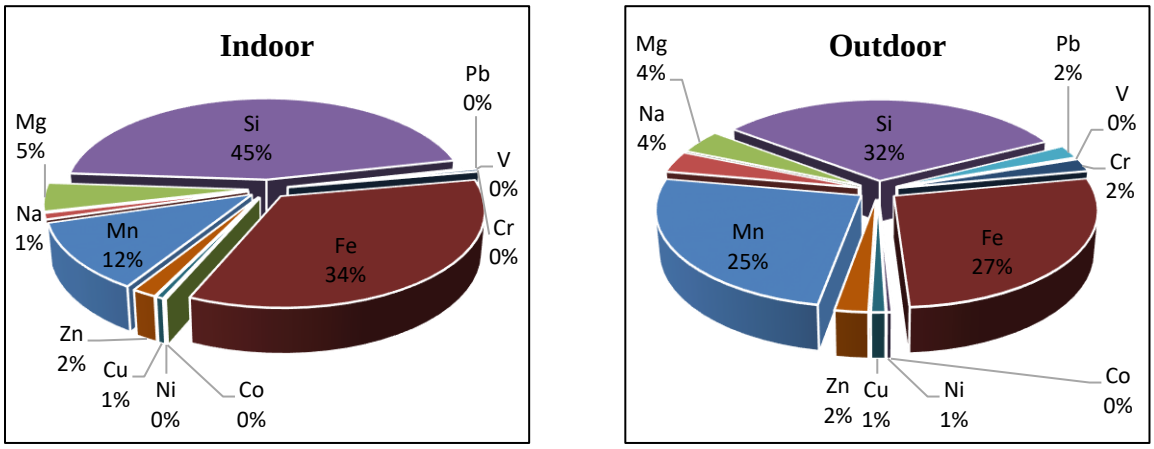


**Figure 9:** Percentage contribution of elements on indoor and outdoor $PM_{2.5}$ sampled across the three residential areas.

# CHAPTER 4: DISCUSSION

This chapter discusses the study results which were then compared to existing literature. The results discussed below include the indoor and outdoor $PM_{2.5}$ mass concentrations obtained gravimetrically and I/O ratios. The descriptive and inferential statistical results are discussed in this chapter. The physical properties of indoor and outdoor $PM_{2.5}$ obtained from SEM and semi-quantitative elemental composition obtained from EDX are also discussed in this chapter. This chapter further discusses the elemental composition of indoor and outdoor $PM_{2.5}$ obtained from ICP-MS. The chapter ends by discussing the limitations and strengths of the study.

## 4.1 Synopsis of study findings

This study provides data about the physicochemical properties of indoor and outdoor $PM_{2.5}$ sampled in selected households at Meyerton. The study aimed to systematically characterise the similarities between indoor and outdoor Mn-bearing $PM_{2.5}$ in three residential areas near a ferromanganese smelter. Outdoor $PM_{2.5}$ mass concentrations were greater than the indoor across the three residential areas. Furthermore, outdoor $PM_{2.5}$ mass concentration was 2.27 fold greater than indoor which agreed with the study's hypothesis. The I/O ratio of 0.44 further indicated that indoor $PM_{2.5}$ mass concentrations were influenced by $PM_{2.5}$ from the outdoor environment. A statistically significant difference was found ($P$=5.8×10$^{-13}$) between indoor and outdoor $PM_{2.5}$ mass concentrations. Indoor $PM_{2.5}$ consisted of irregular and single spherical particles ranging from 0.1 to 0.7 µm in diameter, while outdoor consisted of irregular and agglomerated particles ranging from 0.1 to 1.3 µm in diameter. ICP-MS results indicated that both indoor and outdoor $PM_{2.5}$ were dominated by elements in decreasing order of Si > Fe > Mn > Na > Mg > Zn. However, outdoor $PM_{2.5}$ had the highest concentration of elements.

## 4.2 Indoor and outdoor $PM_{2.5}$ mass concentrations

Table 2 presents a summary of indoor and outdoor $PM_{2.5}$ mass concentrations in Meyerton and it can be observed that outdoor $PM_{2.5}$ mass concentration was greater than indoor. Outdoor $PM_{2.5}$ mass concentration was 2.27 fold greater than indoor. New Sicelo presented the highest average indoor $PM_{2.5}$ mass concentration (12.93 ± 3.29 µg/m$^3$), followed by Old Sicelo (12.25 ± 4.33 µg/m$^3$) and Noldick (7.78 ± 6.08 µg/m$^3$) as shown in Figure 2. Figure 2 also shows that Noldick had the highest average outdoor $PM_{2.5}$ mass concentration (26.23

± 5.02 µg/$m^3$), followed by New Sicelo (24.87 ± 9 µg/$m^3$), and Old Sicelo (18.74 ± 8.86 µg/$m^3$). The indoor and outdoor $PM_{2.5}$ mass concentration findings also support the study hypothesis that outdoor Mn-bearing $PM_{2.5}$ mass concentration would be higher than indoor.

Indoor and outdoor $PM_{2.5}$ mass concentration findings in this study complement those of Hasheminassab *et al.* (2014), Gao *et al.* (2020) and Zhao *et al.* (2020) who found that outdoor $PM_{2.5}$ mass concentrations were significantly higher than the indoor. The high indoor $PM_{2.5}$ mass concentrations at New and Old Sicelo can be attributed to stationary and mobile sources such as the ferromanganese smelter and vehicular emissions. The high indoor $PM_{2.5}$ mass concentrations can also be attributed to the re-suspension of particles through human movements. For instance, re-suspension through walking has been identified as a significant source of indoor PM (Butler, Madhavan and Alper, 2016). The indoor $PM_{2.5}$ could have also been due to dust re-suspended by wind, human activities, and vehicular movement which then enters the indoor environment.

The high indoor $PM_{2.5}$ mass concentration at New and Old Sicelo suggests that the sampled households had many or larger openings whereby the $PM_{2.5}$ infiltrated at a faster rate. Another plausible explanation is that the $PM_{2.5}$ did not only enter through openings but could also be due to foot tracking, cooking, smoking, re-suspension during walking and cleaning activities, and the use of detergents, sprays, and cosmetic products.

Studies by Urso *et al.* (2015) and Kim *et al.* (2018) affirmed that activities such as cooking, incense burning, smoking, and cleaning contribute significantly to the indoor $PM_{2.5}$ mass concentration. The higher indoor $PM_{2.5}$ mass concentration further suggests that the households at New and Old Sicelo had higher room occupancy and human activities (Butler, Madhavan and Alper, 2016). This is further supported by Perrino *et al.* (2016), who found that indoor $PM_{2.5}$ mass concentrations increased significantly when the rooms were occupied, particularly on weekends when the occupants were home.

The lower indoor $PM_{2.5}$ mass concentrations at Noldick suggest that outdoor $PM_{2.5}$ infiltrated at a lower rate. The results are not surprising since most of the sampled households in Noldick were made of brick and cement and had ceilings. The findings support the work of Abdel-Salam (2015) and Delgado-Saborit (2019) who reported that the infiltration of outdoor PM into the indoor environment depends on the characteristics of the structure. Therefore, the different housing structures in New and Old Sicelo and Noldick can explain the variation in indoor $PM_{2.5}$ mass concentrations.

Noldick had the highest outdoor $PM_{2.5}$ mass concentrations relative to Old and New Sicelo, despite that New Sicelo is nearest to the ferromanganese smelter. This finding can be explained by the height of the ferromanganese smelter stack and meteorological conditions. Studies have proven that an emission source with a high stack tends to affect areas that are further away from the source. The outdoor $PM_{2.5}$ mass concentrations at Noldick are also an indication that the ferromanganese smelter is not the only potential emitting source. Therefore, the higher outdoor $PM_{2.5}$ mass concentrations at Noldick can be attributed to vehicular exhaust emissions since the area is next to the smelter and R59 freeway.

The R551 and M61 roads pass through Noldick, Therefore, the higher outdoor $PM_{2.5}$ concentrations can also be attributed to, tyre, and brake PM. Since most of the Noldick area is paved and vegetated, the higher outdoor $PM_{2.5}$ can also be attributed to dust suspended and re-suspended at New and Old Sicelo which is blown by the wind and settles at Noldick. The variation of outdoor $PM_{2.5}$ mass concentrations across the three residential areas could be due to variation in the source, source strength, and different meteorological conditions.

The indoor and outdoor $PM_{2.5}$ mass concentration findings are an indication that indoor $PM_{2.5}$ was influenced by the outdoor. This is supported by the overall I/O ratio of less than 1 as presented in Table 2, which means that indoor was less than the outdoor $PM_{2.5}$ mass concentration. Table 3 shows the I/O ratios of the three residential areas the average I/O ratios at Old Sicelo, New Sicelo, and Noldick were $0.50 \pm 0.07$, $0.54 \pm 0.10$, and $0.27 \pm 0.17$, respectively. From Table 3, it can also be noted that the I/O ratios across the three residential areas are less than 1 which further suggests that indoor was influenced by $PM_{2.5}$ from the outdoor environment (Morawska *et al.*, 2017; Niu *et al.*, 2019; Madureira *et al.*, 2020).

### 4.3 Statistical analysis of indoor and outdoor $PM_{2.5}$ mass concentration

A summary of the statistical results for indoor and outdoor $PM_{2.5}$ mass concentrations in Meyerton is presented in Table 4. A statistically significant difference was found ($P=5.8\times10^{-13}$) between indoor and outdoor $PM_{2.5}$ mass concentrations in Meyerton. This implies that there was a significant difference between the means of indoor and outdoor $PM_{2.5}$ mass concentrations. Table 5 presents a summary of the statistical results between indoor and outdoor $PM_{2.5}$ mass concentrations for the three residential areas. Similarly, a statistically significant difference was found ($P<0.05$) between indoor and outdoor $PM_{2.5}$ mass concentrations across the three residential areas. This also implies that there was a significant

difference between the means of indoor and outdoor $PM_{2.5}$ mass concentrations across the three residential areas.

### 4.4 Morphology of indoor and outdoor $PM_{2.5}$

Figure 3 presents the SEM-EDX for the blank filter and it can be observed that no particles were detected on the filter. Semi-quantitative elemental results from EDX indicated the presence of carbon (56.5%), oxygen (43.4%), and Mn (0.1%), which are the common constituents of PCTE filters. This implies that the filters were not contaminated, thus suitable for sampling.

The representative SEM images of indoor and outdoor $PM_{2.5}$ sampled in the three residential areas are presented in Figure 4 to Figure 6. It can be observed that the particles had different sizes and shapes. SEM revealed that indoor $PM_{2.5}$ at Old Sicelo, New Sicelo, and Noldick consisted of irregular and spherical particles, while outdoor $PM_{2.5}$ consisted of agglomerated and irregular particles. The two microenvironments reported the same or similar morphologies, suggesting that the source of emission is the same for indoor and outdoor $PM_{2.5}$.

In a study conducted near a ferromanganese alloy plant in Cantabria, north of Spain, Hernández-Pellón *et al.* (2017) reported Irregular Mn enriched $PM_{10}$ particles. In their study, Jiang *et al.* (2018) also reported irregular agglomerated particles and concluded that they are due to vehicular emissions and re-suspended dust particles. Therefore, the irregular shape of the indoor and outdoor particles reported in the current study suggests that they are from combustion sources such as motor vehicle engines or the ferromanganese smelter.

The outdoor agglomerated particles are an indication that the particles were of submicron size and agglomerated to form larger particles. These results are consistent with those of Gupta *et al.* (2020), who reported spherical, agglomerated, and irregular particles enriched with elements associated with anthropogenic sources such as industrial activities and vehicular emissions.

It has been well established that spherical particles commonly originate from natural processes such as pollen or anthropogenic sources such as high-temperature combustion processes (Smichowski and Gómez, 2012; Ahmed, Guo and Zhao, 2017). The spherical particles can either exist as single or agglomerated particles (Ahmed, Guo and Zhao, 2017). A study by Gjønnes *et al.* (2011), reported spherical submicron Mn oxide particles that agglomerated to form larger particles which were also observed in the current study.

Although the study by Gjønnes *et al.* (2011) was conducted inside a Mn smelter during various processes it can still be concluded that the indoor spherical particles are from a high combustion source such as the Mn-smelter or motor vehicles (Labrada-Delgado *et al.*, 2012).

A summary of the elemental composition of indoor and outdoor $PM_{2.5}$ for the three residential areas obtained using EDX is presented in Table 6. EDX results indicated that indoor $PM_{2.5}$ sampled at Old Sicelo was dominated by elements in a decreasing order of Si > Al > Fe > S. New Sicelo was dominated by Si > Al > Mn, while indoor $PM_{2.5}$ sampled at Noldick had an abundance of Si > Al > Fe > Ca > S. EDX results also indicated that outdoor $PM_{2.5}$ sampled at Old Sicelo was dominated by Si > Al > Fe > Ca > S. New Sicelo was dominated by Si > Al > Fe > Ca > S > Mn, while the outdoor $PM_{2.5}$ at Noldick was dominated by Si > Al > Fe > S > K > Ca. From Table 6, it can be noted that outdoor $PM_{2.5}$ had the highest concentration of elements.

Potassium is associated with the combustion of solid fuels such as wood and coal, while the other elements are associated with ferromanganese smelters and vehicular emissions (Gholampour *et al.*, 2016). However, elements such as Si, Ca, and Mg are naturally occurring and abundant in the soil. These results are similar to those reported by Hernández-Pellón *et al.* (2017), who used EDX to analyse the elemental composition of $PM_{10}$ particles and reported spherical Mn and Fe enriched particles. However, the elemental concentrations from the EDX are semi-quantitative and small conclusions can be made from such results. Hence in this study, ICP-MS was used to overcome this limitation.

Figure 7 shows the size distribution of indoor and outdoor $PM_{2.5}$ sampled across the three residential areas. The size of indoor particles at Old Sicelo ranged between 0.1 and 1.3 µm while the outdoor particles ranged between 0.1 and 0.7 µm diameter. At New Sicelo indoor particles ranged between 0.1 and 0.7 µm while outdoor particles ranged between 0.1 and 1.1 µm diameter. Indoor particles at Noldick ranged from 0.1 to 0.7 µm while outdoor particles ranged between 0.1 and 0.7 µm in diameter.

Indoor $PM_{2.5}$ across the three residential areas was dominated by particles ranging from a diameter of 0.1 and 0.7 µm while outdoor $PM_{2.5}$ was dominated by particles of 0.1 and 1.3 µm. The particle size findings in this study complement that of Ali *et al.* (2020) who conducted a study in residential areas near a heavily industrialised site in Pakistan. The study reported indoor and outdoor particles ranging from 0.1 to 1.02 µm and 0.1 to 1.6 µm, respectively.

### 4.5 Elemental composition of indoor and outdoor $PM_{2.5}$

The average concentrations of the elements distributed on the sampled indoor and outdoor $PM_{2.5}$ are presented in Figure 8. The average indoor and outdoor Mn concentration was 1.18 µg/m$^3$ and 3.07 µg/m$^3$, respectively. Apart from Mn, other elements selected for the ICP-MS analysis were also detected, however, K and Cd were below the limit of quantification. Surprisingly, the EDX detected Al, however, it was below the limit of quantification of the ICP-MS. Si > Fe > Na > Mg > Zn were the most abundant elements on the indoor and outdoor sampled $PM_{2.5}$. Although both indoor and outdoor $PM_{2.5}$ had an abundance of these elements, outdoor $PM_{2.5}$ had the highest concentration of elements. Similar results have been reported by Wang *et al.* (2019) in dormitories in Nanjing, China. The authors found that the outdoor concentration of elements on $PM_{2.5}$ was higher than the indoor.

The elements reported in the current study have been confirmed to be commonly emitted from ferromanganese smelters (Kero *et al.*, 2019). Studies by Hernández-Pellón *et al.* (2017) and Hernández-Pellón *et al.* (2019) conducted near a ferromanganese alloy plant in Spain also reported an abundance of these elements on ambient $PM_{10}$ samples. Specifically, the authors found an abundance of Mn and Fe enriched $PM_{10}$. The fact that the elemental concentration findings of this study agree with previous studies suggests that the ferromanganese smelter in Meyerton is a major contributing source to ambient air pollution in the three nearby residential areas.

Table 7 presents the elemental composition of indoor and outdoor $PM_{2.5}$ for the three residential areas. Noldick had the highest indoor Mn concentration (1.67 µg/m$^3$), followed by Old Sicelo (1.20 µg/m$^3$), while New Sicelo had the least concentration (1.03 µg/m$^3$). Noldick also had the highest outdoor Mn concentration (6.56 µg/m$^3$), followed by New Sicelo (5.55 µg/m$^3$) and Old Sicelo (3.97 µg/m$^3$). The percentage contribution of the elements on the sampled indoor and outdoor $PM_{2.5}$ across the three residential areas is presented in Figure 9. Similar to the results reported by Jeong *et al.* (2019), outdoor Mn concentration is higher than indoor. The findings also agreed with the study hypothesis that outdoor Mn-bearing $PM_{2.5}$ concentrations would be higher than indoor.

Although Noldick is located furthest from the ferromanganese smelter relative to New Sicelo, it had the highest concentration of elements. The high concentration of Mn at Noldick can be explained by the meteorological conditions during the sampling period. These results are not surprising and agree with previous studies. Studies by Ledoux *et al.* (2006) and Hernández-Pellón *et al.* (2019) conducted around a ferromanganese alloy plant found that

the concentration of elements increased as the distance away from the source increased. Therefore, there is a possibility that the pollutants can be transported further and even change from the air compartment to water and soil.

The increase in the concentration of elements is an indication that the ferromanganese smelter is not the only contributing source. Motor vehicles are also a potential source, this is plausible given that Pb was replaced with Mn as an anti-knock in fuel. Subsequently, motor vehicular emissions are enriched with Mn-bearing and Fe-enriched PM. Moreover, Noldick is nearer the R59 freeway and the M59 which busy roads used by light and heavy motor vehicles.

Iron was detected both in indoor and outdoor $PM_{2.5}$ across the three residential areas and contributed significantly. The high Fe concentrations can be attributed to the ferromanganese smelter, metallurgy industries, and vehicular emissions (Lu *et al.*, 2015; Hernández-Pellón *et al.*, 2017). A study by Sanderson *et al.* (2016) reported that engine blocks can contribute significantly to the ambient Fe concentration and therefore, some of the Fe can be attributed to motor vehicles. However, the Fe can also be attributed to the corrugated Fe used for roofing.

Silicon is a naturally occurring element that is abundant on the earth and the presence of high Si content on the indoor and outdoor $PM_{2.5}$ could be due to the suspension of soil dust by vehicles, wind, and other human activities and release from industrial combustion (Hasheminassab *et al.*, 2014; Gholampour *et al.*, 2016; Zeb *et al.*, 2018). The presence of Cu in indoor and outdoor $PM_{2.5}$ could be due to the combustion of fossil fuels since Cu is an indicator of combustion sources such as coal-burning (Gholampour *et al.*, 2016).

### 4.6 Study limitations

Due to limited funds, only two indoor and outdoor filters per residential area were analysed using ICP-MS. The study did not use a weather monitoring station to obtain meteorological data which are important for the transportation and dispersion of ambient pollutants. Due to this limitation, the $PM_{2.5}$ concentrations are not correlated with meteorological data such as wind speed, wind direction, humidity, and temperature.

Time-activity patterns were also not included in this study. The time-activity patterns would have assisted in the understating of the contribution of indoor sources to the $PM_{2.5}$ mass concentration. The data were collected during the spring period and the emissions are

unlikely to remain consistent throughout the different seasons. Information about the production rate of the smelter was also unobtainable.

The air exchange rate in the sampled household was not measured, it could have helped determine the infiltration and deposition rate of outdoor $PM_{2.5}$ into the indoor environment. Furthermore, the study did not use linear regression to determine the relationship between outdoor and indoor $PM_{2.5}$, instead, only the I/O ratio was used to determine the relationship between indoor and outdoor $PM_{2.5}$.

### 4.7 Study strengths

This is the first study to investigate the physicochemical properties of particulate matter in a residential area near a ferromanganese smelter in South Africa. The study investigated indoor and outdoor $PM_{2.5}$ and did not rely on data from fixed monitoring stations to represent the potential exposure at the level of the receptor. The study also managed to point out the major potential emitting sources of indoor and outdoor Mn-bearing-$PM_{2.5}$. However, additional studies are required to affirm the source or single out one emitting source of indoor and outdoor Mn-bearing $PM_{2.5}$ in Meyerton.

# CHAPTER 5: CONCLUSION

This chapter begins by providing the relevance and significance of the study. Based on the study findings, future research and recommendations are provided. Conclusion and lessons drawn from this study are also provided in this chapter.

## 5.1 Significance of the study

This study investigated the similarities between the physicochemical properties of indoor and outdoor $PM_{2.5}$ sampled in residential areas near a ferromanganese smelter. The average indoor $PM_{2.5}$ mass concentration was 10.99 ± 5.10 µg/m$^3$ while the outdoor was 24.97 ± 6.77 µg/m$^3$. Outdoor $PM_{2.5}$ mass concentration was found to be 2.7 fold greater than indoor which agreed with the study's hypothesis. The I/O ratio was less than 1 supporting the finding that outdoor $PM_{2.5}$ was greater than indoor and that indoor was influenced by $PM_{2.5}$ from the outdoor environment.

Indoor $PM_{2.5}$ had a presence of irregular and agglomerated particles ranging from 0.1–0.7 µm in diameter while $PM_{2.5}$ outdoor also consisted of irregular but single spherical particles ranging from 0.1–1.3 µm in diameter. SEM images indicated that indoor and outdoor $PM_{2.5}$ are from the same or similar emission source. Both indoor and outdoor $PM_{2.5}$ across the three residential areas were dominated by particles of 0.1 µm in diameter.

Indoor and outdoor particles were enriched with Mn and Fe oxides suggesting that they are from a high combustion source such as the Mn smelter or vehicles. Elements commonly emitted from ferromanganese smelters were found on indoor and outdoor $PM_{2.5}$. Mn > Si > Fe > Na > Mg > Zn were the elements found both in indoor and outdoor $PM_{2.5}$, however, outdoor $PM_{2.5}$ had the highest concentration of elements. The findings from this study suggest that motor vehicles and the nearby ferromanganese smelter are major potential emitting sources of Mn-bearing $PM_{2.5}$ in Meyerton.

This is the first study in South Africa to investigate the physicochemical properties of indoor and outdoor $PM_{2.5}$ in a residential area near a ferromanganese smelter. The findings from this study contribute to the understanding of indoor and outdoor $PM_{2.5}$ in residential areas near ferromanganese smelters. The study found that most indoor $PM_{2.5}$ originated from outdoor sources, with the ferromanganese being the main contributing source. Moreover, the $PM_{2.5}$ was enriched with Mn, which can lead to chronic health outcomes amongst vulnerable

groups. The findings can be used to support epidemiological studies where ferromanganese smelters have been associated with neurodegenerative illnesses such as PD.

The findings can be essential for assessing exposure to pollutants associated with ferromanganese smelters located near residential areas. This is important given that the smallest particle size reported in this study is 0.1 µm in diameter which has a high probability of penetrating deeper into the alveolar upon uptake.

### 5.2 Recommendations

Future studies conducting exposure assessment in the Meyerton area are necessary because this study was focused and confined to the characterisation of $PM_{2.5}$. Future studies can investigate the impact of the ferromanganese smelter and motor vehicular emissions beyond the three residential areas studied. Furthermore, future studies can investigate the possibility of the $PM_{2.5}$ changing from the air compartment to water and soil.

Given that the findings of this study suggest the potential for exposure to the Mn-bearing $PM_{2.5}$ both in indoor and outdoor environments. Time-activity pattern studies are necessary to quantify how much time the residents spend indoors, outdoors, and outside the boundaries of their microenvironment. Time-activity pattern studies are necessary since the development of adverse health outcomes depends on the duration of exposure. Therefore, time-activity patterns can be used to collect data that will be useful for exposure assessment and modeling the intake and uptake of $PM_{2.5}$.

Exposure assessment studies can be done by collecting personal concentration in the breathing zone. Breathing zone concentration is suggested to be an accurate estimation of how much the receptor is exposed to relative to ambient and indoor concentration. Future studies should also investigate particle number concentration since this study only reported the mass concentrations of indoor and outdoor $PM_{2.5}$. The bioavailability and bio-accessibility of the Mn-bearing particle should be studied in future studies.

Findings from the current study have indicated that there is a risk of exposure to Mn-bearing $PM_{2.5}$ both in the indoor and outdoor environment. Therefore, there is a need for interventional studies to protect public health. For example, the interventional studies can investigate the type of the interventions needed and where they can be placed to effectively reduce exposure to $PM_{2.5}$ Mn-bearing particles both indoor and outdoor. Interventional studies are important given the health outcomes associated with exposure to Mn-bearing $PM_{2.5}$.

Furthermore, measures are needed to reduce or trap airborne PM in residential areas near smelters. Such measures can include landscape covering with tar, paving, or grass to improve occult deposition. A tree cultivation program can also be initiated, particularly along the road sides as part of an occult deposition programme.

Findings from this study can also be used to conduct a human health risk assessment and environmental impact assessment. The findings can also be useful to future epidemiological studies that want to associate emission from ferromanganese smelters and adverse health outcomes.

Lessons drawn from this study is that there is a need for integrated town planning and industrial development strategies aimed at protecting public health. Therefore, industries such as ferromanganese smelters should be located near residential areas. Conversely, residential areas should also not be developed near such industries, particularly downwind. Residential areas near industries are developed because people want to be closer to their workplace and want to reduce costs associated with transport. Environmental impact studies should be conducted before developing such areas and the potential air quality impacts should be assessed using dispersion models such as Calpuff and Airmod.

# CHAPTER 6: REFERENCES


Abdel-Salam, M. M. M. (2015) 'Investigation of PM2.5 and carbon dioxide levels in urban homes', *Journal of the Air and Waste Management Association*, 65(8), pp. 930–936. doi: 10.1080/10962247.2015.1040138.

Agency for Toxic Substances and Disease Registry (2012) *Toxicological profile for Manganese*. Atlanta, Georgia. Available at: https://www.ncbi.nlm.nih.gov/books/NBK158872/pdf/Bookshelf_NBK158872.pdf (Accessed: 19 February 2019).

Ahmed, M., Guo, X. and Zhao, X.-M. (2017) 'Spectroscopic and microscopic characterization of atmospheric particulate matter', *Instrumentation Science and Technology*, 45(6), pp. 659–682. doi: 10.1080/10739149.2017.1308377.

Aldabe, J. *et al.* (2011) 'Chemical characterisation and source apportionment of PM2.5 and PM10 at rural, urban and traffic sites in Navarra (North of Spain)', *Atmospheric Research*, 102, pp. 191–205. doi: 10.1016/j.atmosres.2011.07.003.

Ali, N. *et al.* (2020) 'Particle size, morphology and characterization of indoor and outdoor airborne particulate matter for toxic metals in Karachi', *International Journal of Environmental Science and Technology*, 17(3), pp. 3969–3982. doi: 10.1007/s13762-020-02771-4.

Allen, J. L. *et al.* (2017) 'Developmental neurotoxicity of inhaled ambient ultrafine particle air pollution: Parallels with neuropathological and behavioral features of autism and other neurodevelopmental disorders', *NeuroToxicology*, 59, pp. 140–154. doi: 10.1016/j.neuro.2015.12.014.

Allen, R. W. *et al.* (2012) 'Modeling the Residential Infiltration of Outdoor PM 2.5 in the Multi-Ethnic Study of Atherosclerosis and Air Pollution (MESA Air)', *Environmental Health Perspectives*, 120(6), pp. 824–830. doi: 10.1289/ehp.1104447.

Alves, C. A. *et al.* (2020) 'Physical and chemical properties of non-exhaust particles generated from wear between pavements and tyres', *Atmospheric Environment*, 224, p. 117252. doi: 10.1016/j.atmosenv.2019.117252.

Amato, F. *et al.* (2016) 'Case Studies of Source Apportionment and Suggested Measures at Southern European Cities', in *Issues in Environmental Science and Technology*, pp. 168–263. doi: 10.1039/9781782626589-00168.

Ammann, A. A. (2007) 'Inductively coupled plasma mass spectrometry (ICP MS): A versatile tool', *Journal of Mass Spectrometry*, pp. 419–427. doi: 10.1002/jms.1206.

Andruska, K. M. and Racette, B. A. (2015) 'Neuromythology of Manganism', *Environmental Epidemiology*, 2, pp. 143–148. doi: 10.1007/s40471-015-0040-x.

Arı, A., Arı, P. E. and Gaga, E. O. (2020) 'Chemical characterization of size-segregated particulate matter (PM) by inductively coupled plasma – Tandem mass spectrometry (ICP-MS/MS)', *Talanta*, 208, p. 120350. doi: 10.1016/j.talanta.2019.120350.

Aschner, J. L. and Aschner, M. (2005) 'Nutritional aspects of manganese homeostasis', *Molecular Aspects of Medicine*, 26(4–5), pp. 353–362. doi: 10.1016/j.mam.2005.07.003.

Aschner, M. *et al.* (2009) 'Manganese and its Role in Parkinson's Disease: From Transport to Neuropathology', *NeuroMolecular Medicine*, 11(4), pp. 252–266. doi: 10.1007/s12017-009-8083-0.

Batterman, S. *et al.* (2011) 'Manganese and lead in children's blood and airborne particulate matter in Durban, South Africa', *Science of The Total Environment*, 409(6), pp. 1058–1068. doi: 10.1016/j.scitotenv.2010.12.017.

Beaupré, L. A. *et al.* (2004) 'Physical and Chemical Characterization of Mn Phosphate/Sulfate Mixture Used in an Inhalation Toxicology Study', *Inhalation Toxicology*, 16(4), pp. 231–244. doi: 10.1080/08958370490277245.

Boudissa, S. M. *et al.* (2006) 'Manganese concentrations in the soil and air in the vicinity of a closed manganese alloy production plant', *Science of The Total Environment*, 361(1–3), pp. 67–72. doi: 10.1016/j.scitotenv.2005.05.001.

Bowler, R. M. *et al.* (2016) 'Environmental exposure to manganese in air: Associations with tremor and motor function', *Science of The Total Environment*, 541, pp. 646–654. doi: 10.1016/j.scitotenv.2015.09.084.

Brodusch, N., Demers, H. and Gauvin, R. (2018) *Field Emission Scanning Electron Microscopy*. Singapore: Springer Singapore (SpringerBriefs in Applied Sciences and Technology). doi: 10.1007/978-981-10-4433-5.

Brüske-Hohlfeld, I. and Peters, A. (2010) 'Epidemiological Studies on Particulate Air Pollution', in *Nanotechnology*. Weinheim, Germany: Wiley-VCH Verlag GmbH & Co. KGaA, pp. 267–290. doi: 10.1002/9783527628155.nanotech018.

Butler, D. A., Madhavan, G. and Alper, J. (eds) (2016) *Health Risks of Indoor Exposure to Particulate Matter, Health Risks of Indoor Exposure to Particulate Matter*. Washington, D.C.: National Academies Press. doi: 10.17226/23531.

Cantone, L. *et al.* (2011) 'Inhalable metal-rich air particles and histone H3K4 dimethylation and H3K9 Acetylation in a Cross-sectional Study of Steel Workers', *Environmental Health Perspectives*, 119(7), pp. 964–969. doi: 10.1289/ehp.1002955.

Carvalho, C. F. de *et al.* (2018) 'Environmental manganese exposure and associations with memory, executive functions, and hyperactivity in Brazilian children', *NeuroToxicology*, 69, pp. 253–259. doi: 10.1016/j.neuro.2018.02.002.

Carvalho, L. da C. (2018) 'Investigation of silver metal clays using Scanning Electron Microscopy with Energy Dispersive Spectroscopy', *International Journal of Conservation Science*, 9(2), pp. 209–218. Available at: www.ijcs.uaic.ro (Accessed: 3 May 2020).

Casuccio, G. S. *et al.* (2004) 'Measurement of fine particulate matter using electron microscopy techniques', *Fuel Processing Technology*, 85(6–7), pp. 763–779. doi: 10.1016/j.fuproc.2003.11.026.

Chen, C. and Zhao, B. (2011) 'Review of relationship between indoor and outdoor particles: I/O ratio, infiltration factor and penetration factor', *Atmospheric Environment*, pp. 275–288. doi: 10.1016/j.atmosenv.2010.09.048.

Chen, P., Culbreth, M. and Aschner, M. (2016) 'Exposure, epidemiology, and mechanism of the environmental toxicant manganese', *Environmental Science and Pollution Research*, 23(14), pp. 13802–13810. doi: 10.1007/s11356-016-6687-0.

Chen, T. *et al.* (2018) 'Relationship between Omnibus and Post-hoc Tests: An Investigation of performance of the F test in ANOVA', *BIOSTATISTICS IN PSYCHIATRY*, 30(1), pp. 60–64. doi: 10.11919/j.issn.1002-0829.218014.

Coetsee, T. (2019) 'The role of manganese ore reduction morphology development in setting reduction mechanisms', *Minerals Engineering journal*, 137, pp. 217–231. doi: 10.1016/j.mineng.2019.04.006.

Colledge, M. A. *et al.* (2015) 'Characterization of air manganese exposure estimates for residents in two Ohio towns', *Journal of the Air & Waste Management Association*, 65(8), pp. 948–957. doi: 10.1080/10962247.2015.1040525.

Cortez-Lugo, M. *et al.* (2018) 'Evaluation of the effect of an environmental management program on exposure to manganese in a mining zone in Mexico', *NeuroToxicology*, 64, pp. 142–151. doi: 10.1016/j.neuro.2017.08.014.

Creamer, M. (2013) 'New R1bn manganese furnace signals beneficiation support – BHP Billiton', *Engineering News and Mining Weekly*, 6 March. Available at: https://m.miningweekly.com/article/new-r1bn-manganese-furnace-signals-support-for-beneficiation-bhp-billiton-2013-03-06 (Accessed: 2 July 2020).

Crenn, V. *et al.* (2018) 'Fine particles sampled at an urban background site and an industrialized coastal site in Northern France—Part 2: Comparison of offline and online analyses for carbonaceous aerosols', *Aerosol Science and Technology*, 52(3), pp. 287–299. doi: 10.1080/02786826.2017.1403008.

Crossgrove, J. and Zheng, W. (2004) 'Manganese toxicity upon overexposure', *NMR in Biomedicine*, 17(8), pp. 544–553. doi: 10.1002/nbm.931.

Davourie, J. *et al.* (2017) 'Evaluation of particulate matter emissions from manganese alloy production using life-cycle assessment', *NeuroToxicology*, 58, pp. 180–186. doi: 10.1016/j.neuro.2016.09.015.

Delgado-Saborit, J. M. (2019) 'Indoor Air as a Contributor to Air Pollution Exposure', in *Issues in Environmental Science and Technology*, pp. 158–195. doi: 10.1039/9781788016179-00158.

Diapouli, E. *et al.* (2011) 'Indoor and outdoor particle number and mass concentrations in Athens. Sources, sinks and variability of aerosol parameters', *Aerosol and Air Quality Research*, 11(6), pp. 632–642. doi: 10.4209/aaqr.2010.09.0080.

Dong, Z. *et al.* (2015) 'Uncertainties in human health risk assessment of environmental contaminants: A review and perspective', *Environment International*, 85, pp. 120–132. doi: 10.1016/j.envint.2015.09.008.

Ellingham, S. T. D., Thompson, T. J. U. and Islam, M. (2018) 'Scanning Electron Microscopy-Energy-Dispersive X-Ray (SEM/EDX): A Rapid Diagnostic Tool to Aid the Identification of Burnt Bone and Contested Cremains', *Journal of Forensic Sciences*, 63(2), pp. 504–510. doi: 10.1111/1556-4029.13541.

Elmes, M. and Gasparon, M. (2017) 'Sampling and single particle analysis for the chemical characterisation of fine atmospheric particulates: A review', *Journal of Environmental Management*, 202, pp. 137–150. doi: 10.1016/j.jenvman.2017.06.067.

Figueiredo Filho, D. B. *et al.* (2013) 'When is statistical significance not significant?', *Brazilian Political Science Review*, 7(1), pp. 31–55. doi: 10.1590/s1981-38212013000100002.

Finkelstein, M. M. and Jerrett, M. (2007) 'A study of the relationships between Parkinson's disease and markers of traffic-derived and environmental manganese air pollution in two Canadian cities', *Environmental Research*, 104, pp. 420–432. doi: 10.1016/j.envres.2007.03.002.

Fulk, F. *et al.* (2017) 'Pathways of inhalation exposure to manganese in children living near a ferromanganese refinery: A structural equation modeling approach', *Science of the Total Environment*, 579, pp. 768–775. doi: 10.1016/j.scitotenv.2016.11.030.

Galvão, E. S. *et al.* (2018) 'Trends in analytical techniques applied to particulate matter characterization: A critical review of fundaments and applications', *Chemosphere*, 199, pp. 546–568. doi: 10.1016/j.chemosphere.2018.02.034.

Gao, X. *et al.* (2020) 'Measurements of indoor and outdoor fine particulate matter during the heating period in Jinan, in North China: Chemical composition, health risk, and source apportionment', *Atmosphere*, 11(9). doi: 10.3390/ATMOS11090885.

Genga, A. *et al.* (2018) 'Individual particle SEM-EDS analysis of atmospheric aerosols in rural, urban, and industrial sites of Central Italy', *Environmental Monitoring and Assessment*, 190(8), p. 456. doi: 10.1007/s10661-018-6826-9.

Gholampour, A. *et al.* (2016) 'Characterization and source identification of trace elements in airborne particulates at urban and suburban atmospheres of Tabriz, Iran', *Environmental Science Pollution Research*, 23, pp. 1703–1713. doi: 10.1007/s11356-015-5413-7.

Gjønnes, K. *et al.* (2011) 'Characterisation of workplace aerosols in the manganese alloy production industry by electron microscopy', *Analytical and Bioanalytical Chemistry*, 399(3), pp. 1011–1020. doi: 10.1007/s00216-010-4470-5.

Gonzalez-Castanedo, Y. *et al.* (2014) 'Size distribution and chemical composition of particulate matter stack emissions in and around a copper smelter', *Atmospheric Environment*, 98, pp. 271–282. doi: 10.1016/j.atmosenv.2014.08.057.

Gozzi, F., Della Ventura, G. and Marcelli, A. (2016) 'Mobile monitoring of particulate matter: State of art and perspectives', *Atmospheric Pollution Research*, 7(2), pp. 228–234. doi: 10.1016/j.apr.2015.09.007.

Gross, J. H. (2017) *Mass Spectrometry*. Cham: Springer International Publishing. doi: 10.1007/978-3-319-54398-7.

GroundWork (2016) *The Destruction of the Highveld: Digging Coal*.

Guo, H. *et al.* (2010) 'Characterization of particle number concentrations and PM2.5 in a school: influence of outdoor air pollution on indoor air', *Environmental Science and Pollution Research*, 17(6), pp. 1268–1278. doi: 10.1007/s11356-010-0306-2.

Gupta, P. *et al.* (2020) 'Exposure to respirable and fine dust particle over North-Central India: chemical characterization, source interpretation, and health risk analysis', *Environmental Geochemistry and Health*, 42(7), pp. 2081–2099. doi: 10.1007/s10653-019-00461-w.

Hänninen, O. and Goodman, P. (2019) 'Outdoor Air as a Source of Indoor Pollution', in *Indoor Air Pollution*, pp. 35–65. doi: 10.1039/9781788016179-00035.

Hasheminassab, S. *et al.* (2014) 'Chemical characterization and source apportionment of indoor and outdoor fine particulate matter (PM 2.5 ) in retirement communities of the Los Angeles Basin', *Science of the Total Environment*, 490, pp. 528–537. doi: 10.1016/j.scitotenv.2014.05.044.

Haynes, E. N. *et al.* (2010) 'Environmental manganese exposure in residents living near a ferromanganese refinery in Southeast Ohio: A pilot study', *NeuroToxicology*, 31(5), pp. 468–474. doi: 10.1016/j.neuro.2009.10.011.

Hermanus, M. A. (2000) ‘Manganese-A Public Health Concern: Its Relevance for Occupational Health and Safety Policy and Regulation in South Africa’, *International Journal of Occupational and Environmental Health*, 6(2), pp. 151–160. doi: 10.1179/oeh.2000.6.2.151.

Hernández-Bonilla, D. *et al.* (2011) ‘Environmental exposure to manganese and motor function of children in Mexico’, *NeuroToxicology*, 32(5), pp. 615–621. doi: 10.1016/j.neuro.2011.07.010.

Hernández-Pellón, A. *et al.* (2017) ‘Characterization of manganese-bearing particles in the vicinities of a manganese alloy plant’, *Chemosphere*, 175, pp. 411–424. doi: 10.1016/j.chemosphere.2017.02.056.

Hernández-Pellón, A. and Fernández-Olmo, I. (2019) ‘Airborne concentration and deposition of trace metals and metalloids in an urban area downwind of a manganese alloy plant’, *Atmospheric Pollution Research*, 10(3), pp. 712–721. doi: 10.1016/j.apr.2018.11.009.

Hoeflinger, W. and Laminger, T. (2019) ‘PM2.5 or respirable dust measurement and their use for assessment of dust separators’, *Journal of the Taiwan Institute of Chemical Engineers*, 94, pp. 53–61. doi: 10.1016/j.jtice.2017.07.035.

Hoek, G. *et al.* (2008) ‘Indoor-outdoor relationships of particle number and mass in four European cities’, *Atmospheric Environment*, 42(1), pp. 156–169. doi: 10.1016/j.atmosenv.2007.09.026.

Hopke, P. K. (2016) ‘Review of receptor modeling methods for source apportionment’, *Journal of the Air & Waste Management Association*, 66(3), pp. 237–259. doi: 10.1080/10962247.2016.1140693.

Horning, K. J. *et al.* (2015) ‘Manganese Is Essential for Neuronal Health’, *Annual Review of Nutrition*, 35(1), pp. 71–108. doi: 10.1146/annurev-nutr-071714-034419.

Hu, J. *et al.* (2015) ‘Source contributions and regional transport of primary particulate matter in China’, *Environmental Pollution*, 207, pp. 31–42. doi: 10.1016/j.envpol.2015.08.037.

Izhar, S. *et al.* (2016) ‘Annual trends in occurrence of submicron particles in ambient air and health risk posed by particle bound metals’, *Chemosphere*, 146, pp. 582–590. doi: 10.1016/j.chemosphere.2015.12.039.

Jeong, C.-H. *et al.* (2019) ‘Indoor measurements of air pollutants in residential houses in urban and suburban areas: Indoor versus ambient concentrations’, *Science of The Total Environment*, 693, p. 133446. doi: 10.1016/j.scitotenv.2019.07.252.

Jiang, N. *et al.* (2018) ‘Characterization of PM 10 and PM 2.5 Source Profiles of Fugitive Dust in Zhengzhou, China’, *Aerosol and Air Quality Research*, 18, pp. 314–329. doi: 10.4209/aaqr.2017.04.0132.

Jin, S.-P. *et al.* (2018) 'Urban particulate matter in air pollution penetrates into the barrier-disrupted skin and produces ROS-dependent cutaneous inflammatory response in vivo', *Journal of Dermatological Science*, 91(2), pp. 175–183. doi: 10.1016/j.jdermsci.2018.04.015.

Karagulian, F. *et al.* (2015) 'Contributions to cities' ambient particulate matter (PM): A systematic review of local source contributions at global level', *Atmospheric Environment*, 120, pp. 475–483. doi: 10.1016/j.atmosenv.2015.08.087.

Kero, I. T. *et al.* (2019) 'Airborne Emissions from Mn Ferroalloy Production', *JOM*, 71(1), pp. 349–365. doi: 10.1007/s11837-018-3165-9.

Khan, M. S. I., Oh, S.-W. and Kim, Y.-J. (2020) 'Power of Scanning Electron Microscopy and Energy Dispersive X-Ray Analysis in Rapid Microbial Detection and Identification at the Single Cell Level', *Scientific Reports*, 10(1), p. 2368. doi: 10.1038/s41598-020-59448-8.

Kim, H., Kang, K. and Kim, T. (2018) 'Measurement of Particulate Matter (PM2.5) and Health Risk Assessment of Cooking-Generated Particles in the Kitchen and Living Rooms of Apartment Houses', *Sustainability*, 10(3), p. 843. doi: 10.3390/su10030843.

Kim, K.-H., Kabir, E. and Kabir, S. (2015) 'A review on the human health impact of airborne particulate matter Human health Particle size', *Environment International*, 74, pp. 136–143. doi: 10.1016/j.envint.2014.10.005.

Koivisto, A. J. *et al.* (2019) 'Source specific exposure and risk assessment for indoor aerosols', *Science of The Total Environment*, 668, pp. 13–24. doi: 10.1016/j.scitotenv.2019.02.398.

Kornblith, E. S. *et al.* (2018) 'Environmental exposure to manganese in air: Tremor, motor and cognitive symptom profiles', *NeuroToxicology*, 64, pp. 152–158. doi: 10.1016/j.neuro.2017.09.012.

Kutchko, B. G. and Kim, A. G. (2006) 'Fly ash characterization by SEM-EDS', *Fuel*, 85(17–18), pp. 2537–2544. doi: 10.1016/j.fuel.2006.05.016.

Kwiecińska, B., Pusz, S. and Valentine, B. J. (2019) 'Application of electron microscopy TEM and SEM for analysis of coals, organic-rich shales and carbonaceous matter', *International Journal of Coal Geology*, 211, p. 103203. doi: 10.1016/j.coal.2019.05.010.

Labrada-Delgado, G. *et al.* (2012) 'Chemical and morphological characterization of PM2.5 collected during MILAGRO campaign using scanning electron microscopy', *Atmospheric Pollution Research*, 3(3), pp. 289–300. doi: 10.5094/APR.2012.032.

Ledoux, F. *et al.* (2006) 'Characterization of iron and manganese species in atmospheric aerosols from anthropogenic sources', *Atmospheric Research*, 82(3–4), pp. 622–632. doi: 10.1016/j.atmosres.2006.02.018.

Lee, E.-Y. *et al.* (2017) 'Welding-related brain and functional changes in welders with chronic and low-level exposure', *NeuroToxicology*, 64, pp. 50–59. doi: 10.1016/j.neuro.2017.06.011.

Lee, S. C. *et al.* (2002) 'Inter-comparison of air pollutant concentrations in different indoor environments in Hong Kong', *Atmospheric Environment*, 36(12), pp. 1929–1940. doi: 10.1016/S1352-2310(02)00176-0.

Li, W. *et al.* (2010) 'Size, composition, and mixing state of individual aerosol particles in a South China coastal city', *Journal of Environmental Sciences*, 22(4), pp. 561–569. doi: 10.1016/S1001-0742(09)60146-7.

Li, X. *et al.* (2017) 'Emission characterization of particulate matter in the ironmaking process', *Environmental Technology*, 40(3), pp. 282–292. doi: 10.1080/09593330.2017.1387180.

Liati, A. *et al.* (2016) 'Electron microscopic characterization of soot particulate matter emitted by modern direct injection gasoline engines', *Combustion and Flame*, 166, pp. 307–315. doi: 10.1016/j.combustflame.2016.01.031.

Lighty, J. S., Veranth, J. M. and Sarofim, A. F. (2000) 'Combustion Aerosols: Factors Governing Their Size and Composition and Implications to Human Health', *Journal of the Air & Waste Management Association*, 50(9), pp. 1565–1618. doi: 10.1080/10473289.2000.10464197.

Loranger, S. and Zayed, J. (1995) 'Environmental and occupational exposure to manganese: a multimedia assessment', *International Archives of Occupational and Environmental Health*, 67(2), pp. 101–110. doi: 10.1007/BF00572233.

Lowther, S. D. *et al.* (2019) 'Particulate Matter Measurement Indoors: A Review of Metrics, Sensors, Needs, and Applications', *Environmental Science and Technology*, 53, pp. 11644–11656. doi: 10.1021/acs.est.9b03425.

Lu, S. *et al.* (2015) 'Physico-chemical characterization of PM2.5 in the microenvironment of Shanghai subway', *Atmospheric Research*, 153, pp. 543–552. doi: 10.1016/j.atmosres.2014.10.006.

Lucchini, R. G. *et al.* (2007) 'High prevalence of parkinsonian disorders associated to manganese exposure in the vicinities of ferroalloy industries', *American Journal of Industrial Medicine*, 50(11), pp. 788–800. doi: 10.1002/ajim.20494.

Lucchini, R. G., Martin, C. J. and Doney, B. C. (2009) 'From Manganism to Manganese-Induced Parkinsonism: A Conceptual Model Based on the Evolution of Exposure', *NeuroMolecular Medicine*, 11(4), pp. 311–321. doi: 10.1007/s12017-009-8108-8.

Lv, Y. *et al.* (2017) 'The Correlation between Indoor and Outdoor Particulate Matter of Different Building Types in Daqing, China', *Procedia Engineering*, 205, pp. 360–367. doi: 10.1016/j.proeng.2017.10.002.

Madureira, J. *et al.* (2020) ‘Assessment of indoor air exposure among newborns and their mothers: Levels and sources of PM10, PM2.5 and ultrafine particles at 65 home environments’, *Environmental Pollution*, 264, p. 114746. doi: 10.1016/j.envpol.2020.114746.

Makonese, T., Meyer, J. and von Solms, S. (2019) ‘Characteristics of spherical organic particles emitted from fixed-bed residential coal combustion’, *Atmosphere*, 10(8), pp. 1–16. doi: 10.3390/atmos10080441.

Malcolm, H. M., Wood, M. and Kingdom, U. (2004) *Concise International Chemical Assessment Document 63. manganese and its compounds: environmental aspects*, *World Health Organization Geneva*. Available at: https://www.who.int/ipcs/publications/cicad/en/CICAD63.pdf (Accessed: 12 July 2019).

Manigrasso, M. *et al.* (2018) ‘Ultrafine particles in domestic environments: Regional doses deposited in the human respiratory system’, *Environment International*, 118, pp. 134–145. doi: 10.1016/j.envint.2018.05.049.

Marris, H. *et al.* (2012) ‘Fast changes in chemical composition and size distribution of fine particles during the near-field transport of industrial plumes’, *Science of The Total Environment*, 427–428, pp. 126–138. doi: 10.1016/j.scitotenv.2012.03.068.

Martins, V. *et al.* (2020) ‘Relationship between indoor and outdoor size-fractionated particulate matter in urban microenvironments: Levels, chemical composition and sources’, *Environmental Research*, 183, p. 109203. doi: 10.1016/j.envres.2020.109203.

Masekameni, D. M. *et al.* (2018) ‘Size Distribution of Ultrafine Particles Generated from Residential Fixed-bed Coal Combustion in a Typical Brazier’, *Aerosol and Air Quality Research*, 18, pp. 2618–2632. doi: 10.4209/aaqr.2018.03.0105.

Masekameni, M. D. *et al.* (2020) ‘Morphology and elemental analysis of freshly emitted particles from packed-bed domestic coal combustion’, *Clean Air Journal*, 30(2), pp. 1–10. doi: 10.17159/caj/2020/30/2.8582.

Mazzei, F. *et al.* (2008) ‘Characterization of particulate matter sources in an urban environment’, *Science of The Total Environment*, 401(1–3), pp. 81–89. doi: 10.1016/j.scitotenv.2008.03.008.

McDonald, R. and Biswas, P. (2004) ‘A Methodology to Establish the Morphology of Ambient Aerosols’, *Journal of the Air & Waste Management Association*, 54(9), pp. 1069–1078. doi: 10.1080/10473289.2004.10470986.

Menezes-Filho, J. A. *et al.* (2009) ‘High levels of hair manganese in children living in the vicinity of a ferro-manganese alloy production plant’, *NeuroToxicology*, 30(6), pp. 1207–1213. doi: 10.1016/j.neuro.2009.04.005.

Menezes-Filho, J. A. *et al.* (2014) 'Elevated manganese exposure and school-aged children's behavior: A gender-stratified analysis', *NeuroToxicology*, 45, pp. 293–300. doi: 10.1016/j.neuro.2013.09.006.

Miah, M. R. *et al.* (2020) 'The effects of manganese overexposure on brain health', *Neurochemistry International*, 135, p. 104688. doi: 10.1016/j.neuint.2020.104688.

Michalke, B. and Fernsebner, K. (2014) 'New insights into manganese toxicity and speciation', *Journal of Trace Elements in Medicine and Biology*, 28(2), pp. 106–116. doi: 10.1016/j.jtemb.2013.08.005.

Monn, C. (2002) 'Chapter 4 Exposure assessment of air pollutants: a review on spatial heterogeneity and indoor/outdoor/personal exposure to suspended particulate matter, nitrogen dioxide and ozone', in *Developments in Environmental Science*, pp. 117–182. doi: 10.1016/S1474-8177(02)80007-9.

Morawska, L. *et al.* (2013) 'Indoor aerosols: From personal exposure to risk assessment', *Indoor Air*, 23(6), pp. 462–487. doi: 10.1111/ina.12044.

Morawska, L. *et al.* (2017) 'Airborne particles in indoor environment of homes, schools, offices and aged care facilities: The main routes of exposure', *Environment International*, 108, pp. 75–83. doi: 10.1016/j.envint.2017.07.025.

Moreno, T. *et al.* (2011) 'Manganese in the urban atmosphere: identifying anomalous concentrations and sources', *Environmental Science and Pollution Research*, 18(2), pp. 173–183. doi: 10.1007/s11356-010-0353-8.

Mukherjee, A. and Agrawal, M. (2017) 'World air particulate matter: sources, distribution and health effects', *Environmental Chemistry Letters*, 15, pp. 283–309. doi: 10.1007/s10311-017-0611-9.

Myers, J. E. *et al.* (2003) 'Nervous System Effects of Occupational Manganese Exposure on South African Manganese Mineworkers', *NeuroToxicology*, 24, pp. 649–656. doi: 10.1016/S0161-813X(03)00035-4.

Nascimento, S. *et al.* (2016) 'Associations among environmental exposure to manganese, neuropsychological performance, oxidative damage and kidney biomarkers in children', *Environmental Research*, 147, pp. 32–43. doi: 10.1016/j.envres.2016.01.035.

Niu, J. *et al.* (2010) 'Evaluation of airborne particulate matter and metals data in personal, indoor and outdoor environments using ED-XRF and ICP-MS and co-located duplicate samples', *Atmospheric Environment*, 44(2), pp. 235–245. doi: 10.1016/j.atmosenv.2009.10.009.

Niu, X. *et al.* (2019) 'Characterization of chemical components and cytotoxicity effects of indoor and outdoor fine particulate matter (PM2.5) in Xi'an, China', *Environmental Science and Pollution Research*, 26(31), pp. 31913–31923. doi: 10.1007/s11356-019-06323-3.

O'Neal, S. L. and Zheng, W. (2015) 'Manganese Toxicity Upon Overexposure: a Decade in Review', *Current Environmental Health Reports*, 2(3), pp. 315–328. doi: 10.1007/s40572-015-0056-x.

Oberdörster, G. and Kuhlbusch, T. A. J. (2018) 'In vivo effects: Methodologies and biokinetics of inhaled nanomaterials', *NanoImpact*, 10, pp. 38–60. doi: 10.1016/j.impact.2017.10.007.

Omrani, M. *et al.* (2017) 'Assessment of atmospheric trace metal deposition in urban environments using direct and indirect measurement methodology and contributions from wet and dry depositions', *Atmospheric Environment*, 168, pp. 101–111. doi: 10.1016/j.atmosenv.2017.08.064.

Otero-Pregigueiro, D. *et al.* (2018) 'Estimation of PM10-bound manganese concentration near a ferromanganese alloy plant by atmospheric dispersion modelling', *Science of the Total Environment*, 627, pp. 534–543. doi: 10.1016/j.scitotenv.2018.01.246.

Otero-Pregigueiro, D. and Fernández-Olmo, I. (2018) 'Use of CALPUFF to predict airborne Mn levels at schools in an urban area impacted by a nearby manganese alloy plant', *Environment International*, 119, pp. 455–465. doi: 10.1016/j.envint.2018.07.005.

Ou, S. Y. *et al.* (2018) 'Effect of manganese on neural endocrine hormones in serum of welders and smelters', *Journal of Trace Elements in Medicine and Biology*, 50, pp. 1–7. doi: 10.1016/j.jtemb.2018.05.018.

Pallarés, S. *et al.* (2019) 'The relationship between indoor and outdoor levels of PM10 and its chemical composition at schools in a coastal region in Spain', *Heliyon*, 5(8), p. e02270. doi: 10.1016/j.heliyon.2019.e02270.

Pallarés, S. *et al.* (2020) 'Morphological Characterization of Indoor Airborne Particles in Seven Primary Schools', *International Journal of Environmental Research and Public Health*, 17(9), p. 3183. doi: 10.3390/ijerph17093183.

Panda, S. and Shiva Nagendra, S. M. (2018) 'Chemical and morphological characterization of respirable suspended particulate matter (PM10) and associated heath risk at a critically polluted industrial cluster', *Atmospheric Pollution Research*, 9(5), pp. 791–803. doi: 10.1016/j.apr.2018.01.011.

Park, M. *et al.* (2018) 'Differential toxicities of fine particulate matters from various sources', *Scientific Reports*, 8(1), p. 17007. doi: 10.1038/s41598-018-35398-0.

Parmalee, N. L. and Aschner, M. (2016) 'Manganese and aging', *NeuroToxicology*, 56, pp. 262–268. doi: 10.1016/j.neuro.2016.06.006.

Parsons-White, A. B. and Spitzer, N. (2018) 'Environmentally relevant manganese overexposure alters neural cell morphology and differentiation in vitro', *Toxicology in Vitro*, 50, pp. 22–28. doi: 10.1016/j.tiv.2018.02.015.

Pavilonis, B. T. *et al.* (2015) 'Manganese concentrations in soil and settled dust in an area with historic ferroalloy production', *Journal of Exposure Science & Environmental Epidemiology*, 25(4), pp. 443–450. doi: 10.1038/jes.2014.70.

Peres, T. V *et al.* (2016) '"Manganese-induced neurotoxicity: a review of its behavioral consequences and neuroprotective strategies"', *BMC Pharmacology and Toxicology*, 17(1), p. 57. doi: 10.1186/s40360-016-0099-0.

Perrino, C., Tofful, L. and Canepari, S. (2016) 'Chemical characterization of indoor and outdoor fine particulate matter in an occupied apartment in Rome, Italy', *Indoor Air*, 26(4), pp. 558–570. doi: 10.1111/ina.12235.

Peters, A. *et al.* (2006) 'Translocation and potential neurological effects of fine and ultrafine particles a critical update', *Particle and Fibre Toxicology*, 3(13). doi: 10.1186/1743-8977-3-13.

Popoola, L. T. *et al.* (2018) 'Assessment of atmospheric particulate matter and heavy metals: a critical review', *International Journal of Environmental Science and Technology*, 15(5), pp. 935–948. doi: 10.1007/s13762-017-1454-4.

Pöschl, U. (2010) *Composition, Transformation and Effects of Nanoparticles in the Atmosphere*, *Nanotechnology*. doi: 10.1002/9783527628155.nanotech016.

Pröfrock, D. and Prange, A. (2012) 'Inductively coupled plasma-mass spectrometry (ICP-MS) for quantitative analysis in environmental and life sciences: A review of challenges, solutions, and trends', *Applied Spectroscopy*, pp. 843–868. doi: 10.1366/12-06681.

Racette, B. A. *et al.* (2018) 'A screening tool to detect clinical manganese neurotoxicity', *NeuroToxicology*, 64(2016), pp. 12–18. doi: 10.1016/j.neuro.2017.02.009.

Riediker, M. *et al.* (2019) 'Particle toxicology and health - where are we?', *Particle and Fibre Toxicology*, 16(1), p. 19. doi: 10.1186/s12989-019-0302-8.

Riffault, V. *et al.* (2015) 'Fine and Ultrafine Particles in the Vicinity of Industrial Activities: A Review Fine and Ultrafine Particles in the Vicinity of Industrial Activities: A Review', *Critical Reviews in Environmental Science and Technology*, 45(21), pp. 2305–2356. doi: 10.1080/10643389.2015.1025636.

Rodrigues, J. L. *et al.* (2018) 'Airborne manganese exposure and neurobehavior in school-aged children living near a ferro-manganese alloy plant', *Environmental Research*, 167(May), pp. 66–77. doi: 10.1016/j.envres.2018.07.007.

Rodríguez-Agudelo, Y. *et al.* (2006) 'Motor alterations associated with exposure to manganese in the environment in Mexico', *Science of The Total Environment*, 368(2–3), pp. 542–556. doi: 10.1016/j.scitotenv.2006.03.025.

Rodríguez, S. *et al.* (2007) 'A study on the relationship between mass concentrations, chemistry and number size distribution of urban fine aerosols in Milan, Barcelona and London', *Atmospheric Chemistry and Physics*, 7(9), pp. 2217–2232. doi: 10.5194/acp-7-2217-2007.

Rohra, H. *et al.* (2018) 'Indoor-outdoor association of particulate matter and bounded elemental composition within coarse, quasi-accumulation and quasi-ultrafine ranges in residential areas of northern India', *Science of The Total Environment*, 631–632, pp. 1383–1397. doi: 10.1016/j.scitotenv.2018.03.095.

Sajani, Z. S. *et al.* (2015) 'Spatial and indoor/outdoor gradients in urban concentrations of ultrafine particles and PM 2.5 mass and chemical components', *Atmospheric Environment*, 103, pp. 307–320. doi: 10.1016/j.atmosenv.2014.12.064.

Salma, I. *et al.* (2015) 'Lung burden and deposition distribution of inhaled atmospheric urban ultrafine particles as the first step in their health risk assessment', *Atmospheric Environment*, 104, pp. 39–49. doi: 10.1016/j.atmosenv.2014.12.060.

Sammut, M. L. *et al.* (2010) 'Speciation of Cd and Pb in dust emitted from sinter plant', *Chemosphere*, 78(4), pp. 445–450. doi: 10.1016/j.chemosphere.2009.10.039.

Sanderson, P. *et al.* (2016) 'Characterisation of iron-rich atmospheric submicrometre particles in the roadside environment', *Atmospheric Environment*, 140, pp. 167–175. doi: 10.1016/j.atmosenv.2016.05.040.

dos Santos, N. R. *et al.* (2019) 'Manganese exposure and association with hormone imbalance in children living near a ferro-manganese alloy plant', *Environmental Research*, 172, pp. 166–174. doi: 10.1016/j.envres.2019.02.021.

Satsangi, P. G. and Yadav, S. (2014) 'Characterization of PM2.5 by X-ray diffraction and scanning electron microscopy–energy dispersive spectrometer: its relation with different pollution sources', *International Journal of Environmental Science and Technology*, 11(1), pp. 217–232. doi: 10.1007/s13762-012-0173-0.

Setyan, A. *et al.* (2019) 'Investigation on the near-field evolution of industrial plumes from metalworking activities', *Science of the Total Environment*, 668, pp. 443–456. doi: 10.1016/j.scitotenv.2019.02.399.

Sielicki, P. *et al.* (2011) 'The progress in electron microscopy studies of particulate matters to be used as a standard monitoring method for air dust pollution', *Critical Reviews in Analytical Chemistry*, pp. 314–334. doi: 10.1080/10408347.2011.607076.

Sly, P. D. *et al.* (2016) 'Health Consequences of Environmental Exposures: Causal Thinking in Global Environmental Epidemiology', *Annals of Global Health*, 82(1), p. 3. doi: 10.1016/j.aogh.2016.01.004.

Smichowski, P. and Gómez, D. R. (2012) 'Atmospheric Aerosols, Analysis of', in *Encyclopedia of Analytical Chemistry*. Chichester, UK: John Wiley & Sons, Ltd. doi: 10.1002/9780470027318.a9338.

Smith, D. *et al.* (2007) 'Biomarkers of Mn exposure in humans', *American Journal of Industrial Medicine*, 50(11), pp. 801–811. doi: 10.1002/ajim.20506.

Solís-Vivanco, R. *et al.* (2009) 'Cognitive impairment in an adult Mexican population non-occupationally exposed to manganese', *Environmental Toxicology and Pharmacology*, 28(2), pp. 172–178. doi: 10.1016/j.etap.2009.04.001.

Squizzato, S. *et al.* (2018) 'A long-term source apportionment of PM2.5 in New York State during 2005–2016', *Atmospheric Environment*, 192, pp. 35–47. doi: 10.1016/j.atmosenv.2018.08.044.

Stanislawska, M. *et al.* (2017) 'Coarse, fine and ultrafine particles arising during welding - Analysis of occupational exposure', *Microchemical Journal*, 135, pp. 1–9. doi: 10.1016/j.microc.2017.06.021.

Statistics South Africa (2011) *Statistics South Africa*. Available at: http://www.statssa.gov.za/?page_id=4286&id=11181 (Accessed: 20 October 2019).

Stebounova, L. V *et al.* (2018) 'Physicochemical properties of air discharge-generated manganese oxide nanoparticles: Comparison to welding fumes', *Environmental Science: Nano*, 5(3), pp. 696–707. doi: 10.1039/c7en01046j.

Steenkamp, J. D. *et al.* (2018) 'Working towards an increase in manganese ferroalloy production in South Africa - A research agenda', *Journal of the Southern African Institute of Mining and Metallurgy*. doi: 10.17159/2411-9717/2018/v118n6a13.

Steenkamp, J. D. and Basson, J. (2013) 'The manganese ferroalloys industry in southern Africa', *Journal of the Southern African Institute of Mining and Metallurgy*, 113, pp. 667–676.

Steyn, L. (2018) 'South32 reviews future of smelter amid higher power prices', *BusinessDay*, 18 July. Available at: https://www.businesslive.co.za/bd/companies/mining/2019-07-18-south32-reviews-future-of-smelter-amid-higher-power-prices/ (Accessed: 2 July 2020).

Thompson, J. E. (2018) *Airborne Particulate Matter: Human Exposure and Health Effects, Journal of Occupational and Environmental Medicine*. doi: 10.1097/JOM.0000000000001277.

Turpin, B. J. *et al.* (2007) 'Relationships of Indoor, Outdoor, and Personal Air (RIOPA): part II. Analyses of concentrations of particulate matter species.', *Research report (Health Effects Institute)*, (130 Pt 2).

Ul-Hamid, A. (2018) *A Beginners' Guide to Scanning Electron Microscopy*. Cham: Springer International Publishing. doi: 10.1007/978-3-319-98482-7.

Urso, P. *et al.* (2015) 'Identification of particulate matter determinants in residential homes', *Building and Environment*, 86, pp. 61–69. doi: 10.1016/j.buildenv.2014.12.019.

Valavanidis, A., Fiotakis, K. and Thomas, V. (2008) 'Airborne Particulate Matter and Human Health: Toxicological Assessment and Importance of Size and Composition of Particles for Oxidative Damage and Carcinogenic Mechanisms', *Journal of Environmental Science and Health*, 26(4), pp. 339–362. doi: 10.1080/10590500802494538.

Verenice Muñoz-Rocha, T. *et al.* (2018) 'Prenatal co-exposure to manganese and depression and 24-months neurodevelopment', *NeuroToxicology*, 64, pp. 134–141. doi: 10.1016/j.neuro.2017.07.007.

Viana, M. (2013) *Urban Air Quality in Europe*. Edited by M. Viana. Berlin, Heidelberg: Springer Berlin Heidelberg (The Handbook of Environmental Chemistry). doi: 10.1007/978-3-642-38451-6.

Walsh, M. P. (2007) 'The global experience with lead in gasoline and the lessons we should apply to the use of MMT', *American Journal of Industrial Medicine*, 50(11), pp. 853–860. doi: 10.1002/ajim.20483.

Wang, F. *et al.* (2019) 'Heavy metal characteristics and health risk assessment of PM2.5 in students' dormitories in a university in Nanjing, China', *Building and Environment*, 160, p. 106206. doi: 10.1016/j.buildenv.2019.106206.

Weisel, C. P. *et al.* (2005) 'Relationship of Indoor, Outdoor and Personal Air (RIOPA) study: study design, methods and quality assurance/control results', *Journal of Exposure Science & Environmental Epidemiology*, 15(2), pp. 123–137. doi: 10.1038/sj.jea.7500379.

Wild, P., Bourgkard, E. and Paris, C. (2009) 'Lung cancer and exposure to metals: The epidemiological evidence', in *Methods in Molecular Biology*, pp. 139–167. doi: 10.1007/978-1-60327-492-0_6.

World Health Organization (2016) *Ambient air pollution: A global assessment of exposure and burden of disease*. Geneva. Available at: https://www.who.int/phe/publications/air-pollution-global-assessment/en/ (Accessed: 6 February 2020).

Wu, D. *et al.* (2017) 'Chemical characterization and toxicity assessment of fine particulate matters emitted from the combustion of petrol and diesel fuels', *Science of the Total Environment*, pp. 172–179. doi: 10.1016/j.scitotenv.2017.06.058.

Xing, Y. and Brimblecombe, P. (2019) 'Role of vegetation in deposition and dispersion of air pollution in urban parks', *Atmospheric Environment*, 201, pp. 73–83. doi: 10.1016/j.atmosenv.2018.12.027.

Young, T., Myers, J. E. and Thompson, M. Lou (2005) 'The Nervous System Effects of Occupational Exposure to Manganese-Measured as Respirable Dust-in a South African Manganese Smelter', *NeuroToxicology*, 26, pp. 993–1000. doi: 10.1016/j.neuro.2005.05.002.

Yue, W. *et al.* (2006) 'Characterization of PM2.5 in the ambient air of Shanghai city by analyzing individual particles', *Science of The Total Environment*, 368(2–3), pp. 916–925. doi: 10.1016/j.scitotenv.2006.03.043.

Yue, W. *et al.* (2008) 'Source apportionment of ambient fine particle size distribution using positive matrix factorization in Erfurt, Germany', *Scienece of the Total Environment*, 398, pp. 133–144. doi: 10.1016/j.scitotenv.2008.02.049.

Zanetti-Ramos, B. G. *et al.* (2010) 'Characterization of polymeric particles with electron microscopy, dynamic light scattering, and atomic force microscopy', *Particulate Science and Technology*, 28(5), pp. 472–484. doi: 10.1080/02726351.2010.504133.

Zeb, B. *et al.* (2018) 'On the morphology and composition of particulate matter in an urban environment', *Aerosol and Air Quality Research*, 18(6), pp. 1431–1447. doi: 10.4209/aaqr.2017.09.0340.

Zhang, H. *et al.* (2019) 'Multiple exposure pathways and health risk assessment of heavy metal(loid)s for children living in fourth-tier cities in Hubei Province', *Environment International*, 129, pp. 517–524. doi: 10.1016/j.envint.2019.04.031.

Zhao, J. *et al.* (2020) 'Particle Mass Concentrations and Number Size Distributions in 40 Homes in Germany: Indoor-to-outdoor Relationships, Diurnal and Seasonal Variation', *Aerosol and Air Quality Research*, 20, pp. 576–589. doi: 10.4209/aaqr.2019.09.0444.

Zhou, L. *et al.* (2019) 'Investigation on the relationship of droplet atomization performance and fine particle abatement during the chemical agglomeration process', *Fuel*, 245, pp. 65–77. doi: 10.1016/j.fuel.2019.02.033.

Zota, A. R. *et al.* (2011) 'Metal sources and exposures in the homes of young children living near a mining-impacted Superfund site', *Journal of Exposure Science and Environmental Epidemiology*, 21(5), pp. 495–505. doi: 10.1038/jes.2011.21.

# Appendix A: Plagiarism declaration form


PLAGIARISM DECLARATION TO BE SIGNED BY ALL HIGHER DEGREE STUDENTS

SENATE PLAGIARISM POLICY: APPENDIX ONE

I **SETLAMORAGO JACKSON THOBEJANE** (Student number: **2281450**) am a student registered for the degree of **MASTER OF SCIENCE IN EXPOSURE SCIENCE** in the academic year **2021**.

I hereby declare the following:

- I am aware that plagiarism (the use of someone else's work without their permission and/or without acknowledging the original source) is wrong.
- I confirm that the work submitted for assessment for the above degree is my own unaided work except where I have explicitly indicated otherwise.
- I have followed the required conventions in referencing the thoughts and ideas of others.
- I understand that the University of the Witwatersrand may take disciplinary action against me if there is a belief that this is not my own unaided work or that I have failed to acknowledge the source of the ideas or words in my writing.

Signature: Thobejane SJ Date: **23 June 2021**

# Appendix B: Research ethics clearance certificate

UNIVERSITY OF THE WITWATERSRAND, JOHANNESBURG

R14/49 Prof Gill Nelson et al

**HUMAN RESEARCH ETHICS COMMITTEE (MEDICAL)**

**CLEARANCE CERTIFICATE NO. M150466**

| | |
|---|---|
| **NAME: (Principal Investigator)** | Prof Gill Nelson et al |
| **DEPARTMENT:** | School of Public Health<br>Meyerton (Gauteng) and Potchefstroom (North West),<br>South Africa |
| **PROJECT TITLE:** | Motor and Cognitive Health Outcomes in a Manganese-Exposed African Community |
| **DATE CONSIDERED:** | 24/04/2015 (Initial approval 15/06/2015) |
| **DECISION:** | Approved unconditionally |
| **CONDITIONS:** | Protocol amendment (including change of study site) |
| **SUPERVISOR:** | |
| **APPROVED BY:** | Professor CB Penny, Chairperson, HREC (Medical) |
| **DATE OF APPROVAL:** | 04/09/2018 |

**This clearance certificate is valid for 5 years from date of approval. Extension may be applied for.**

**DECLARATION OF INVESTIGATORS**

To be completed in duplicate and **ONE COPY** returned to the Research Office Secretary on the Third Floor, Faculty of Health Sciences, Phillip Tobias Building, 29 Princess of Wales Terrace, Parktown, 2193, University of the Witwatersrand. I/we fully understand the conditions under which I am/we are authorized to carry out the above-mentioned research and I/we undertake to ensure compliance with these conditions. Should any departure be contemplated, from the research protocol as approved, I/we undertake to resubmit the application to the Committee. **I agree to submit a yearly progress report**. The date for annual re-certification will be one year after the date of convened meeting where the study was initially reviewed. In this case, the study was initially reviewed in **April** and will therefore be due in the month of **April** each year. Unreported changes to the application may invalidate the clearance given by the HREC (Medical).

Principal Investigator Signature Date

**PLEASE QUOTE THE PROTOCOL NUMBER IN ALL ENQUIRIES**

# Appendix C: Data capturing sheet

Date: _____

**Sample number/ ID:** _____

**Time**

Start time: _____ End time: _____

**Weather condition**

| Day 1 | Day 2 | Day 3 | Day 4 | Day 5 | Day 6 | Day 7 |
|---|---|---|---|---|---|---|
| | | | | | | |

***Sunny: 1 Windy: 2 Cloudy: 3 Rainy 4**

---

**Pump flow rate**

Pre- flow rate: _____ Post flow rate: _____

**Filter mass**

Pre mass: _____ Post mass: _____

---

**Additional information:**

_____
_____
_____
_____
_____
_____

**Details of the data collector**

Name & Surname: _____ Cell number: _____

# Appendix D: Standard operating procedures

**Preparation of filters**

- The filters were conditioned for 24 hours before and after weighing

**During the preparation of filters, the conditions of the weighing room were as follows:**

- Sterile environment
- The temperature ranged between 21–22˚C
- The humidity was between 35–37%
- There was no cross ventilation in the room

**Quality checks**

- Ensure that the working surfaces are clean and free from dust
- Switch on the microbalance scale (Sartorius, CPA 225D)
- Allow the microbalance scale to condition for 30 minutes
- Weigh the standard pendulums of 100 and 200 g on the microbalance before and after sampling to calibrate the scale and to validate the results.
- Wear powder-free latex gloves

**Consumables**

- Forceps
- Filter cassette
- Filters
- Ghost wipes
- Powder-free latex gloves
- Cyclone

**Weighing procedure**

- Ensure the microbalance doors are tightly closed
- Ensure that the reading on the microbalance scale is zero
- Use forceps to remove the PCTE filter from the filter holder
- Use the hand to open the door of the microbalance scale
- Gently place the filter onto the microbalance scale
- Gentle close the microbalance doors and ensure they are tightly closed
- View the mass of the display screen
- Allow the scale to stabilize
- Record the mass

- Remove the filter and re-weigh three times using the same procedure as described above
- If the mass does not vary significantly, calculate the average filter mass and record it on the datasheet
- Transfer the filter into the filter cassette
- Place and store the cassettes in a cooler box

**Pump calibration**

- The flow rate must be set at 2.75L/m

**Procedure for calibrating the flow rate:**

- Place the pump on a flat and stable table that is not disturbed
- Connect the tube to the inlet of the pump then connect the tube to the outlet of the cassette. Connect the tube of the inlet of the cassette, then to the outlet of the gilibrator (Figure 10).
- Use a soap dispenser for flow estimation
- Pour the soap dispenser into the inlet of the gilibrator

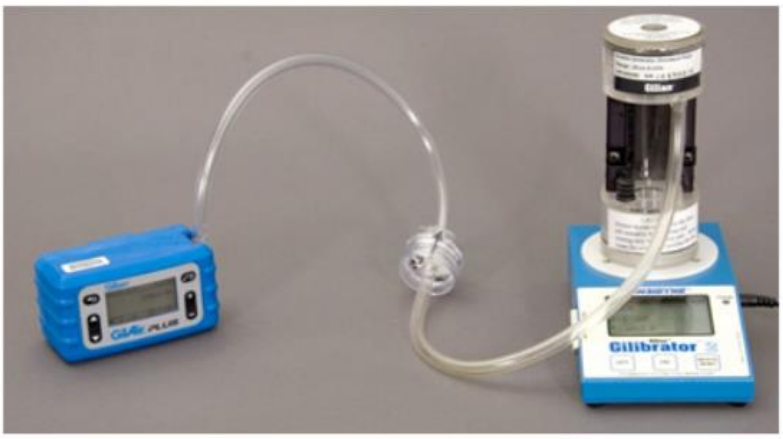


**Figure 10:** Calibration train

**Operation**

- Switch on the gilibrator
- Switch on the pump
- Press the black button on the gilibrator to generate a bubble. Repeat the process three times and record the estimated flow rate on the display screen
- Record the average flow rate and compare it with the flow rate of 2.75L/m
- Use the crew driver provided by the manufacturer to adjust the flow rate to 2.75L/m

- Record the flow rate into the datasheet pre flow rate
- Disconnect the calibration sampling train
- Pack the gilibrator

**Field sampling**

- Place the pump in the allocated space of the selected houses
- Connect the sampling tube of one meter in length
- Attach the $PM_{2.5}$ cyclone (Gs-3 multiple-inlet cyclone) into the inlet of the sampling cassette

**Attachment of cyclone:**

- Remove the third ring of the sampling cassette inlet
- Attach the $PM_{2.5}$ cyclone
- Connect the sampling tube to the outlet of the sampling cassette (Figure 11)
- Attach the cyclone coupled with the cassette to the sampling holder inside and outside the house


**Figure 11:** Sampling train

**Selection of sampling location**

- The sampling location indoor must be selected to ensure the non-disturbance of the samplers due to household movements. The sampler must be placed at a height of ~1.5 meters above the ground
- The selection of the outdoor sampling location must be at the roof height attached to the building wall
- The outdoor sampler must be towards the windward direction of the smelter.

- Record the meteorological conditions in the data collection sheet
- Connect the pump to an electric power supply
- Switch on the pump and record the starting time
- Check the pump after every second day to ensure it is still in operation
- On the $7^{th}$ day, switch off the pump and record the time
- Remove the sampling cassette together with the cyclone
- Remove the cyclone and fit in the inlet ring
- Use the cassette caps to close the inlet and outlet of the cassette
- Place the samples into a cooler box
- Transport the samples to the laboratory within 24 hours.